Musgrave Province, South Australia: Processing and inversion of regional airborne electromagnetic (AEM) data

Camilla Soerensen, Tim Munday, Tania Ibrahimi,
Kevin Cahill, and Mat Gilfedder

Goyder Institute for Water Research
Technical Report Series No. 18/06

www.goyderinstitute.org

Goyder Institute for Water Research Technical Report Series ISSN: 1839-2725

The Goyder Institute for Water Research is a partnership between the South Australian Government through the Department for Environment and Water, CSIRO, Flinders University, the University of Adelaide, the University of South Australia and the International Centre of Excellence in Water Resource Management. The Institute enhances the South Australian Government's capacity to develop and deliver science-based policy solutions in water management. It brings together the best scientists and researchers across Australia to provide expert and independent scientific advice to inform good government water policy and identify future threats and opportunities to water security.

Enquires should be addressed to: Goyder Institute for Water Research
Level 4, 33 King William Street
Adelaide, SA 5000
tel: 08 8236 5200
e-mail: enquiries@goyderinstitute.org

Citation

Soerensen, C.C., Munday, T.J., Ibrahimi, T., Cahill, K. and Gilfedder, M. (2018) *Musgrave Province, South Australia: Processing and inversion of regional airborne electromagnetic (AEM) data.* Goyder Institute for Water Research Technical Report Series No. 18/06

Contents

Figures

Tables

Executive summary

The Geological Survey of South Australia (GSSA) and the Department for Environment and Water (DEW) invested in the acquisition of new regional airborne electromagnetic (AEM) data covering the Musgrave Province in South Australia. The purpose of these surveys was, in part, to identify potential palaeovalley hosted groundwater resources that could help secure water supplies for remote communities and support potential mineral resource developments, as well as development opportunities such as the pastoral industry.

The AEM method, being non-invasive, fast and effective, particularly in remote areas where access on the ground can be challenging, can assist in mapping the location and geometry of aquifer systems including palaeovalleys, which constitute an important groundwater resource for local communities, industry and environment.

The primary objectives of the work carried out for this report were, as part of the Goyder Institute's GFLOWS-3 Project:

1. To assess and process data from the two regional-scale AEM surveys, covering a significantly larger part of the Musgrave Province, and;
2. To invert these two AEM data sets using a common approach to deliver a seamless model of the subsurface conductivity structure taking account of the survey area and specifications of each system employed.

This report briefly reviews details of the AEM systems employed and the survey specifications used in this extended study of the Musgrave Province. It principally focuses on detailing the processing applied to the data and the results from their subsequent inversion.

Two different AEM surveys were planned with a relatively wide line spacing of 2 km, wide enough to cover a large region, whilst being close enough to provide useful information about the variability of cover, including the location and geometry of the major palaeovalley systems known to be present in the area. Both surveys were flown with a line spacing of 2 km in a north-south direction. The western survey was flown with the TEMPEST high moment (HM) system, and the eastern part with the SkyTEM^{312FAST} system. Both systems are time domain AEM systems, one being of a fixed wing configuration (TEMPEST), the other being helicopter borne (SkyTEM). The orientation of the survey boundaries and their extent was defined in consultation with key stakeholders in the region, including State Government departments, the community and industry.

The processing and subsequent inversion of the TEMPEST and SkyTEM data was carried out using the AarhusInv one-dimensional (1D) processing and inversion code. The processing procedure applied to the two datasets differed due to the nature of the raw data provided by the contractors. The two surveys were inverted using a smooth layer model employing lateral constraints and for the finer scale survey areas a spatially constrained inversion approach was employed.

The inverted products of two regional AEM surveys, acquired by different systems, have been merged to provide a regional-scale image of the palaeovalley systems that characterise the Musgrave Province. The orientation and distribution of the palaeovalley fill is represented as a conductive sedimentary sequence, which overlies a very resistive basement. The derived conductivity structure appears well determined by a 1D layered earth inversion. The conductivity pattern and by inference, the palaeovalleys shows a close affinity with the basement structure of the province, indicating its significance in determining the original drainage systems. The observed conductivity structure also shows a close correspondence with the alluvial sequences defined in the GFLOWS-1 hydrogeological framework map, indicating that the original conceptualisation, based on combining information from a contemporary terrain index (MrVBF) and local-scale airborne electromagnetic data acquired for mineral exploration in the region, was well founded.

Acknowledgments

The work described here was undertaken through the support of the South Australian Government's Goyder Institute and CSIRO. The continued support of the South Australian Department for Environment and Water, particularly Adrian Costar and Mark Keppel and Neil Power is acknowledged. The work would also not have been possible without the support of the Geological Survey of South Australia (GSSA) through the PACE Cu initiative.

1 Introduction

1.1 Background

The Goyder Institute's Facilitating Long-Term Outback Water Solutions Stage 3 (G-Flows Stage-3) Project is primarily concerned with the validation of the regional hydrogeological framework methodology developed in projects G-Flows Stages 1 (see Munday et al. 2013). It also seeks to extend that framework to provide a regional groundwater resource assessment in a data poor area through the integration of regional geophysical and geological data coupled with targeted hydrogeological data acquisition (principally through drilling) and interpretation. These objectives will be met by developing a three-dimensional geological model of the unconfined aquifer systems in the Anangu Pitjantjatjara Yankunytjatjara (APY) Lands and the Musgrave Province using regional geophysical coverage.

Research outcomes for G-Flows Stage-3 include workflows for defining groundwater resources, conceptual models of aquifer systems and groundwater quality for community, industry and environment in remote areas characterised by a paucity of data. These workflows will have application in other parts of South Australia, and elsewhere in Australia where knowledge of the groundwater resources is limited. In the APY Lands it will also deliver a regional-scale resource assessment, providing a framework for determining sustainable groundwater use across a substantive part of the region.

Part of the G-Flows Stage-3 project will extend the scientific approaches undertaken in the preceding stages 1 and 2, where in the former, legacy airborne electromagnetic (AEM) data acquired by mineral explorers were re-interpreted to develop a hydrogeological framework (and produce a Hydrogeological Framework Map for the Musgrave Province) to help define the groundwater resource potential of the region (see Munday et al. 2013). The Geological Survey of South Australia (GSSA) and the Department for Environment and Water (DEW) have invested in the acquisition and processing of new AEM data, which covers the Musgrave Province in South Australia (Figure 1). The purpose of this study was to identify potential palaeovalley hosted groundwater resources that could help secure water supplies for remote communities and support potential mineral resource developments, as well as development opportunities such as the pastoral industry.

1.2 Objectives

Employing two airborne electromagnetic systems to acquire data over a large part of the Musgrave Province in South Australia presents the opportunity to significantly extend information about the subsurface in an otherwise data poor area. The AEM method, being non-invasive, fast and effective, particularly in remote areas where access on the ground can be challenging, can assist in mapping the location and geometry of aquifer systems including palaeovalleys, which constitute an important groundwater resource for local communities, industry and environment.

The primary objectives of the work carried out for this report were:

1. To assess and process data from the two regional-scale AEM surveys, covering a significantly larger part of the Musgrave Province, and;
2. To invert these two AEM data sets using a common approach to deliver a seamless model of the subsurface conductivity structure taking account of the survey area and specifications of each system employed.

This report briefly reviews details of the AEM systems employed and the survey specifications used in this extended study of the Musgrave Province. It principally focuses on detailing the processing applied to the data and the results from their subsequent inversion. The results presented here are derived from an unconstrained (in the sense of being linked to external data - borehole/surface or other measurement) inversion of the data.

1.3 Musgrave Province airborne electromagnetic surveys

For the State Government regional AEM data acquisition, two different AEM surveys were planned with a relatively wide line spacing of 2 km, wide enough to cover a large region, whilst being close enough to provide useful information about the variability of cover, including the location and geometry of the major palaeovalley systems known to be present in the area. Both surveys were flown with a line spacing of 2 km in a north-south direction. The western survey was flown with the TEMPEST high moment (HM) system, and the eastern part with the SkyTEM^{312FAST} system (Figure 1). Both systems are time domain AEM systems, one being of a fixed wing configuration (TEMPEST), the other being helicopter borne (SkyTEM). The orientation of the survey boundaries and their extent was defined in consultation with key stakeholders in the region, including State Government departments, the community and industry.

Acquisition, quality assurance and quality control of the two AEM surveys was managed by Geoscience Australia (GA) on behalf of the Geological Survey of South Australia (GSSA) and CSIRO using their standard protocols. Survey specifications (system type, line orientation and spacing) was determined through discussion between the GSSA, the Department for Environment and Water (DEW), CSIRO, and GA, guided by a desire to resolve regolith thickness and understand regional variations in regolith stratigraphy.

The survey area was divided into two separate parts with a small overlap – one overlapping line where the surveys join. Both surveys were flown with a line spacing of 2 km in a north-south direction. The 8595 line-kilometres of TEMPEST HM data were acquired between the 18th of August and 17th of September 2016 by CGG Aviation Pty. Ltd., while the 8412 line-kilometres of SkyTEM^{312FAST} data were acquired between 9th September and 13th of October 2016. In addition to the 2 km line spacing, SkyTEM data were also acquired in smaller infill areas where the line spacing was reduced to 250 and 500 m to map finer details in these areas (Figure 2).

1.4 Rationale for two different airborne electromagnetic systems

The rationale for selecting two different systems for the extended coverage of the Musgrave Province was linked to cost and to the need to acquire spatial information at scales appropriate to the targets of interest.

In the western region, the aim was to acquire information relating to basement geology and cover, the latter being of an undetermined thickness and conductivity. The presence of the Lindsay palaeochannel (Alley and Lindsay 1995), interpreted as a sediment-filled major trunk drainage system that runs through the Musgrave Province from north to south was also a target, although little was known of the thickness of the cover within it, or its conductivity. The serendipitous targeting of deep conductors was also considered in the choice of systems. With these points in mind, the fixed-wing TEMPEST high moment (HM) AEM system was selected, potentially providing good signal to noise in areas of conductive cover, whilst also providing the moment required to explore deeper. In the eastern region, the focus was on acquiring information on the aquifer systems present, particularly in the vicinity of the indigenous communities. For this reason, the SkyTEM^{312FAST} AEM system was selected.

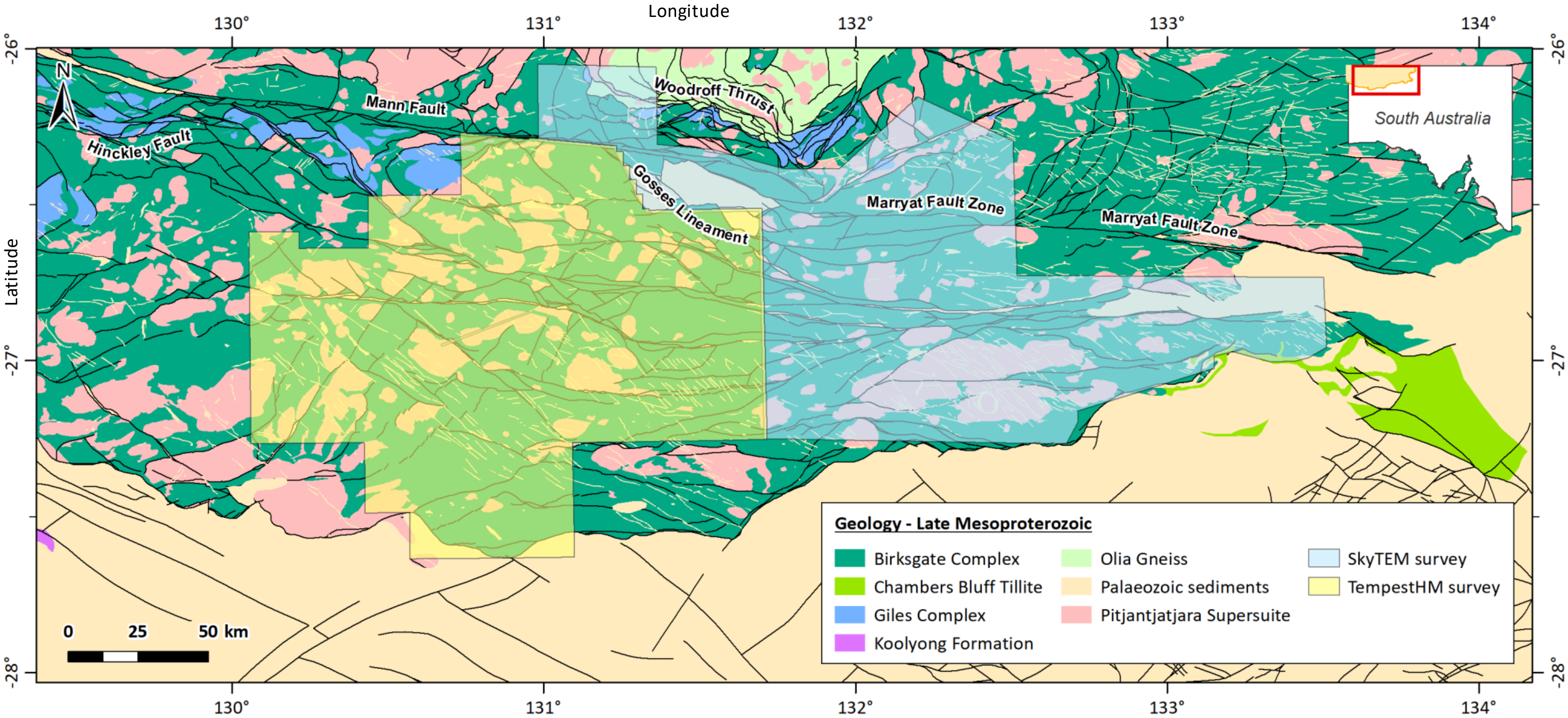

Figure 1. Location of the TEMPEST High Moment (HM) (western) and the SkyTEM surveys (eastern) overlaid on interpreted bedrock geology of the Musgrave Province. The location of existing AEM data sets acquired for mineral exploration purposes is also shown.

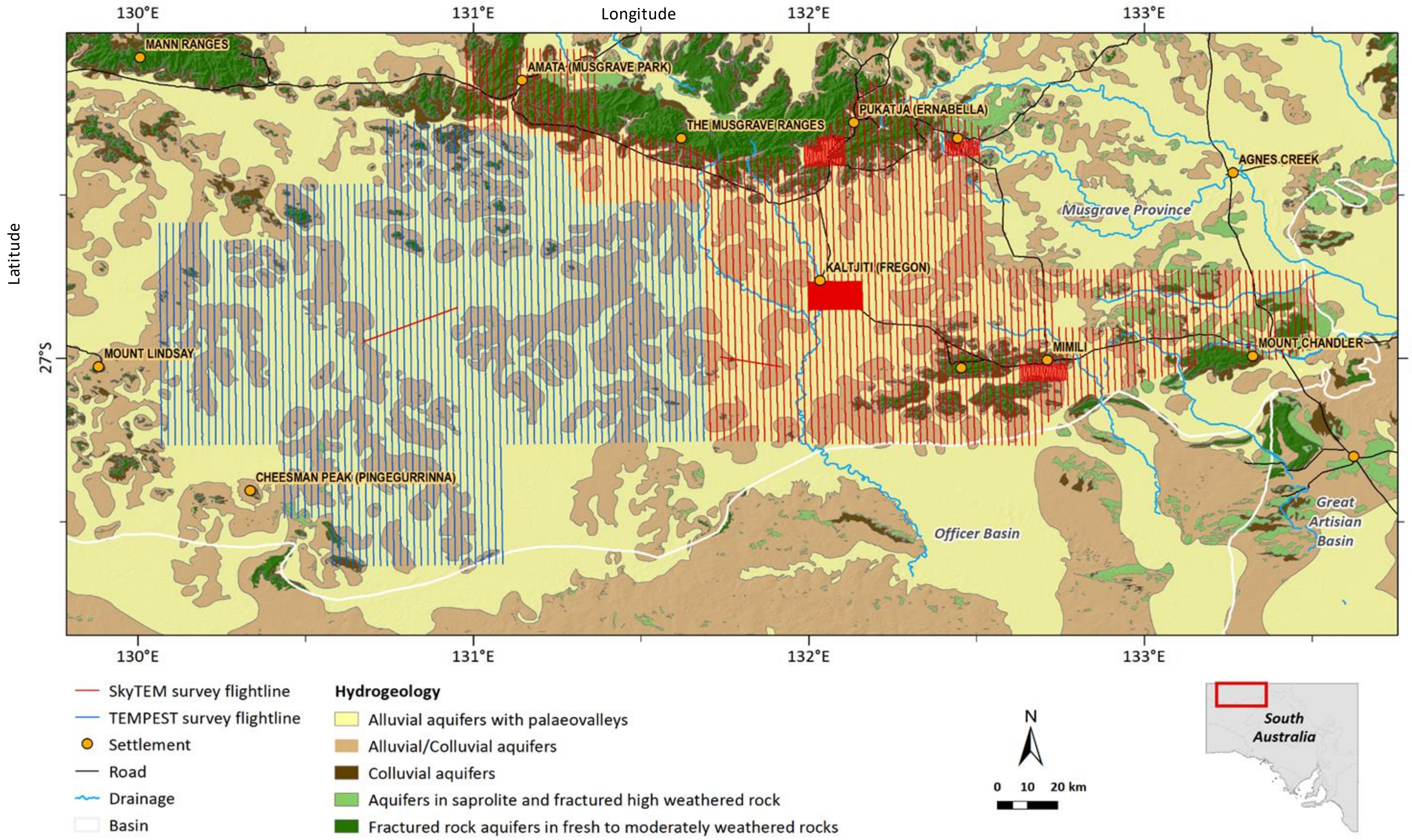

Figure 2. The flight line orientation map for the regional Musgrave Province airborne electromagnetic surveys. Flight lines are overlain on a hydrogeological framework map (Munday et al. 2013) for the region.

2 Airborne electromagnetic data acquisition

2.1 Time domain airborne electromagnetic principles

Electromagnetic surveying techniques involve the measurement of the varying response of the ground due to the propagation of electromagnetic fields. Primary fields are generated by passing a current through a loop or coil, referred to as the transmitter loop, which in turn generates a magnetic field - the primary field (see Figure 3). When the current in the transmitter is turned off abruptly, an electrical current is induced in the ground which will results in another magnetic field, the secondary field. As time passes the resistance in the ground will weaken these induced currents, resulting in a decaying secondary magnetic field which is measured by the receiver coils (positioned at the rear, and offset from the transmitter loop in the SkyTEM system, or in a towed bird, below and to the rear of the aircraft in the TEMPEST system (see Figures 4 and 5). The receiver coils record the response of a decaying signal in the ground at various times (referred to as gates or time windows) after the transmitter pulse has been switched off (Peters 2001). These time windows are typically logarithmically increasing to improve the signal to noise ratio at later times.

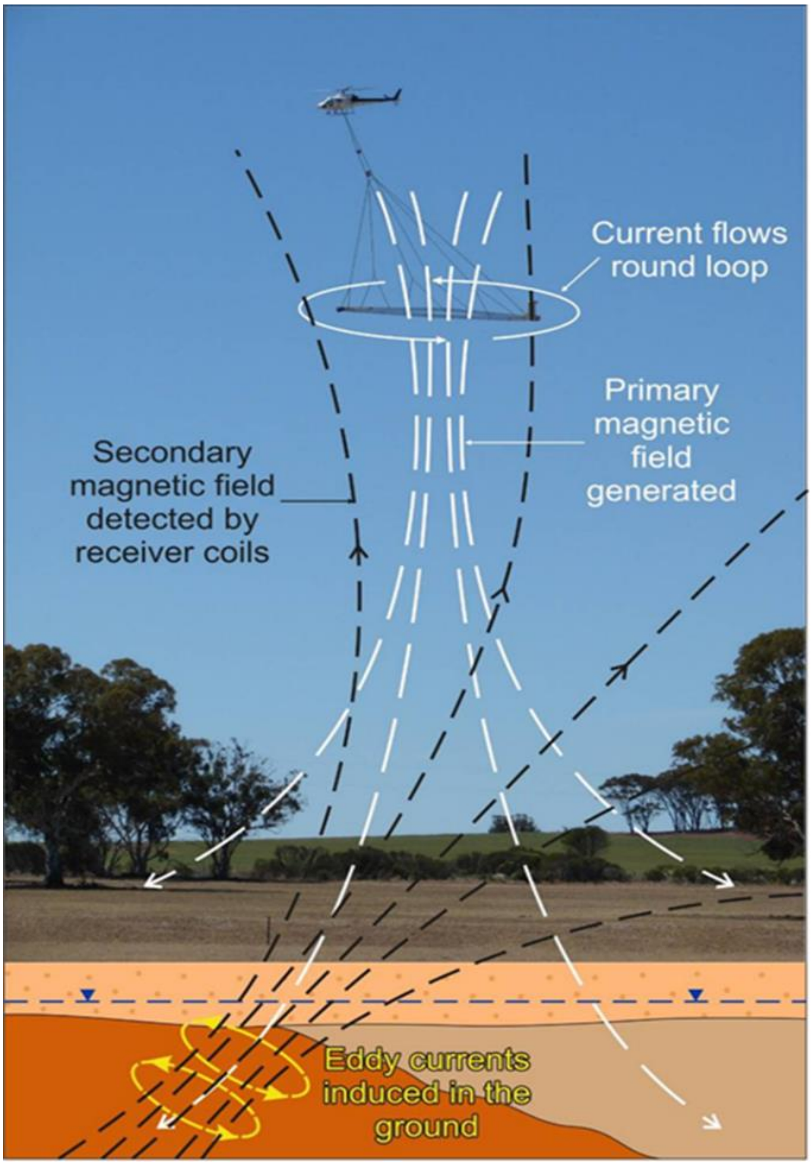

Figure 3. Operating principles of a time domain electromagnetic system.

Just after turn-off of the transmitter current, the current in the ground will be near surface and therefore the measured signal will reflect conductivities of near surface layers. At later times the current propagates deeper into the ground and the measured signal will contain information of the conductivity of these deeper layers. As the induced current results from the magnetic component of the electromagnetic field there is no need to have physical contact between transmitter or receiver and the ground.

The difference between the transmitted (primary) and received (secondary) electromagnetic fields will be determined by the geometry and electrical properties of conductors in the ground. Materials that are highly conductive produce strong secondary electromagnetic fields. Sediments (alluvium), soils or other regolith materials that contain saline pore water generate such fields. The shape of the decaying signal provides information about the vertical conductivity structure of the subsurface.

Most AEM systems map contrasts in ground conductivity that are then interpreted on the basis of experience and with the support of ancillary data, including surface and bore water salinity (electrical conductivity), downhole conductivity measurements, lithology logs from drilling, surface geophysical investigations and other observations.

3 Airborne electromagnetic systems

3.1 The TEMPEST High Moment airborne electromagnetic system

The TEMPEST system is a fixed-wing time domain airborne electromagnetic system developed in 1998 by Cooperative Research Centre for Australian Mineral Exploration Technologies (CRC-AMET) established by the Australian Government's cooperative research centres program (Lane and Pracilio 2000). The system has been widely used in Australia for both prospect-scale surveys (Beckitt 2003), catchment management (Lane et al. 2001) and groundwater mapping (Sattel and Kgotlhang 2004). It has also been deployed for surveys covering large regional areas, including, for example, the Paterson in Western Australia (WA), Pine Creek in the Northern Territory, the Frome Embayment in South Australia, and the Capricorn region of WA (Roach 2010, 2012; Craig 2011 and Ley-Cooper et al. 2017). These surveys have formed part Australian State and Federal Government initiatives involving the acquisition of pre-competitive data to encourage mineral exploration in "greenfield" areas.

The TEMPEST system (Lane et al. 2000) uses a fixed-wing aircraft as the platform where the transmitter loop is draped around the wingtips, tail and nose of the aircraft while the receiver coil is hosted in a bird towed approximately 120 m behind and 40 m below the aircraft (Figure 4).

Figure 4. TEMPEST electromagnetic system in survey mode.

The transmitter height is typically nominally 120 m above the ground. The system measures both the inline (Z) and the vertical (X) components. The deconvolved ground response is converted to a 100% duty cycle square-wave B-field response. More detailed system specifications can be found in Table 1 and 2 and in the acquisition and logistics report provided by CGG (CGG 2016). The TEMPEST HM system, as configured on a Casa 212 fixed wing platform, differed from the standard TEMPEST and the newer 208 platform as detailed in Table 3. The most significant differences are reflected in differences in the Peak current and moment. In the context of the G-Flows Stage-3 Project these properties would benefit the definition of thick conductive cover.

Table 1: Table detailing TEMPEST High Moment system specifications

SYSTEM	HIGH MOMENT TEMPEST	
Base frequency (Hz)	25	
Tx peak current (A)	1200	
Tx loop area (m^2)	240	
Transmitter turns	1	
Peak moment (Am^2)	288000	
Average moment (Am^2)	144000	
Waveform	Square	
Duty cycle	50%	
Transmitter pulse width and off time	10 ms	10 ms
Time gates (µs)	13-16200	
Tx-Rx horizontal separation	115 m (nominal)	
Tx-Rx vertical separation	47 m (nominal)	
Receiver components	X & Z	
Stacked data output interval	200 ms (~12 m)	
Flying height (m)	120	

Table 2: Window specifications for the TEMPEST high moment (HM) system

WINDOW	GATE START (µS)	GATE CENTER (µS)	GATE END (µS)
1	7	13	20
2	33	40	47
3	60	67	73
4	87	107	127
5	140	173	207
6	220	280	340
7	353	453	553
8	567	720	873
9	887	1120	1353
10	1367	1733	2100
11	2113	2693	3273
12	3287	4200	5113
13	5127	6560	7993
14	8007	10,200	12393
15	12,407	16,200	19,993

Table 3: System specifications for the various TEMPEST systems

TEMPEST System	STANDARD	HIGH MOMENT	208
Base frequency	75/25 Hz	25 Hz	25/12.5 Hz
Transmitter area	244 m^2	244 m^2	154 m^2
Transmitter turns	1	1	1
Waveform	Square	Square	Square
Duty cycle	50%	50%	50%
Transmitter pulse width	10 ms	10 ms	10 ms
Transmitter off-time	10 ms	10 ms	10 ms
Transmitter turnoff	42 µs	80 µs	~ 55 µs
Peak current	280 A	1,200 A	560 A
Peak moment	68,320 Am^2	288,000 Am^2	86,240 Am^2
Average moment	34,160 Am^2	144,000 Am^2	43,120 Am^2
Sample rate	75 kHz on X and Z	75 kHz on X and Z	76.8 kHz (X and Z)
Sample interval	13 microseconds	13 microseconds	13 microseconds
Samples per half-cycle	1500	1500	1536
System bandwidth	25 Hz to 37.5 kHz	25 Hz to 37.5 kHz	25 Hz to 38.4 kHz
Nominal Flying Height (subject to safety considerations)	120 m	120 m	100-120 m
EM sensor	Towed bird -3 component dB/dt coils	Towed bird - 3 component dB/dt coils	Towed bird - 3 component dB/dt coils
Tx-Rx horizontal separation	117 m (nominal)	117 m (nominal)	115 m (nominal)
Tx-Rx vertical separation	41.5 m (nominal)	41.5 m (nominal)	45 m (nominal)
Stacked data output interval	200 ms (~12 m)	200 ms (~12 m)	200 ms (~12 m)
Number of output windows	15	15	15
Window centre times	13 µs to 16.2 ms	13 µs to 16.2 ms	13.3 µs to 16.2 ms

3.2 The SkyTEM airborne electromagnetic system

The SkyTEM system were deployed in the Musgrave Province; was the SkyTEM^{312FAST}. The SkyTEM system is a time domain helicopter-borne system developed in Denmark in 2004 (see Sørensen and Auken 2003 and Halkjaer et al. 2006 for a more complete technical description). The system was originally developed for groundwater mapping purposes and in an Australian context the SkyTEM system has successfully been applied to mapping of alluvial aquifers, including buried palaeovalley systems, across Australia (see, for example, Viezzoli et al. 2009; Lawrie et al. 2010; Fitzpatrick et al. 2011, Davis et al. 2015, 2016, and Munday et al. 2016), as well as for minerals exploration (see, for example, Reid and Viezzoli 2007, and Ley Cooper et al. 2014).

The SkyTEM carries the transmitter loop and receiver coil as a sling load beneath the helicopter (Figure 5). The system is capable of operating in a dual transmitter mode; a low moment with a low current and high base frequency provides early time data for shallow imaging, and a high moment mode, with a higher current and a lower base frequency provides late time data for deeper imaging.

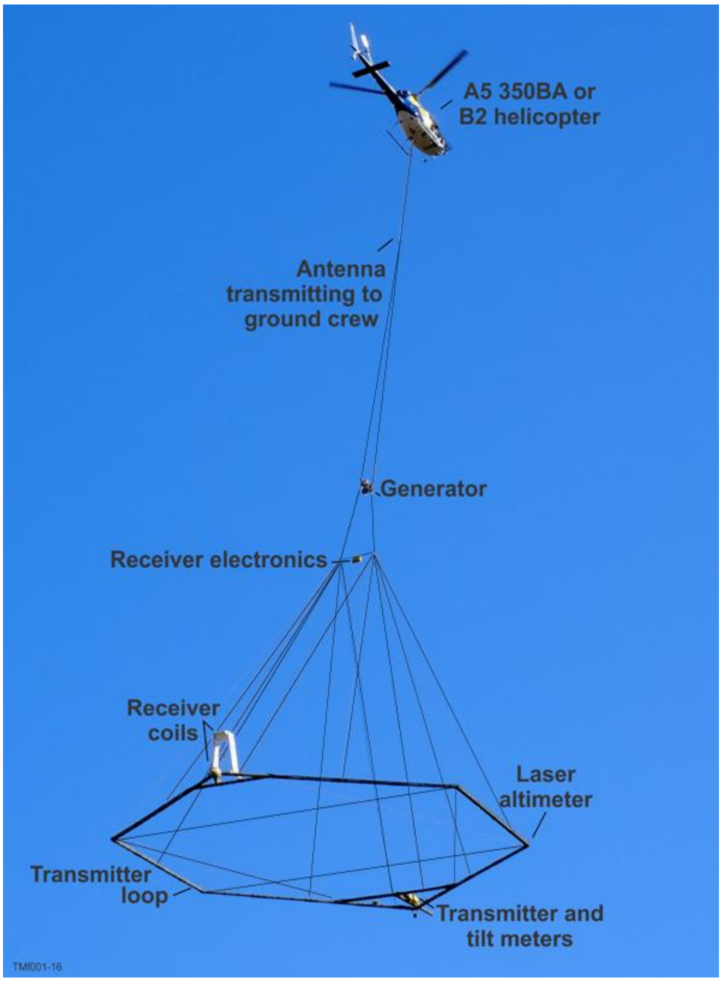

Figure 5. SkyTEM^{312FAST} in survey mode.

The receiver coils are rigidly positioned at the rear of the transmitter frame and slightly above it in a near null position relative to the primary field. Additional details are provided in Tables 4, 5 and 6, and in the acquisition and processing report (SkyTEM 2016).

Table 4: SkyTEM^{312FAST} AEM system specifications

SYSTEM	SKYTEM LOW MOMENT	SKYTEM HIGH MOMENT
Base frequency (Hz)	275	25
Tx peak current (A)	5.9	117
Tx loop area (m^2)	337	337
Transmitter turns	2	12
Peak moment (Am^2)	3980	473000
Waveform	Linear rise, linear ramp-off, bipolar	Pseudo-rectangular, linear ramp-off, bipolar
Duty cycle (%)	44	25
Transmitter on time (ms)	0.8	5
Transmitter off time (ms)	1.018	15
Time gates (µs)	16.42–877	392.4–13160
Front gate (µs)	0	370
Receiver components	X & Z	X & Z
Flying height (m)	45	45

3.3 Spatial resolution of airborne electromagnetic systems

The spatial resolution or footprint of an AEM system is the area or volume of the ground beneath the system which contributes the majority of the response. The spatial resolution of an AEM system depends on the scale of the system, transmitted power and frequency range, receiver sensitivity and ground conductivity distribution (Reid et al. 2006). The footprint of a system can also be used to assess appropriate flight line spacing for surveys as well as the applicability of one-dimensional (1D) interpretations. The resolution is better along lines where data density is large compared to across lines.

The ability of the helicopter-borne systems to fly lower (transmitter and receiver at around 30 m above the ground) compared to the fixed wing systems where the transmitter is at a height of 100 m does increase the resolution and the potential depth of investigation particularly in resistive terrains. In conductive terrains low flying systems are better able to penetrate the conductive overburden (Macnae 2007).

Table 5: Window specifications for the SkyTEM^{312FAST} Low Moment

WINDOW	GATE START (µS)	GATE CENTER (µS)	GATE END (µS)
9	14.63	16.415	18.2
10	18.63	20.915	23.2
11	23.63	26.415	29.2
12	29.63	33.415	37.2
13	37.63	42.415	47.2
14	47.63	53.915	60.2
15	60.63	68.415	76.2
16	76.63	86.415	96.2
17	96.63	108.915	121.2
18	121.63	136.915	152.2
19	152.63	172.415	192.2
20	193.63	217.915	243.2
21	243.63	274.915	306.2
22	306.63	346.415	387.2
23	387.63	437.915	488.2
24	488.63	551.915	615.2
25	615.63	695.915	776.2
26	776.63	877.415	978.2

Table 6: Window specifications for the SkyTEM^{312FAST} High Moment

WINDOW	GATE START (µS)	GATE CENTER (µS)	GATE END (µS)
13	387.63	392.415	397.2
14	397.63	403.915	410.2
15	410.63	418.415	426.2
16	426.63	436.415	446.2
17	446.63	458.915	471.2
18	471.63	486.915	502.2
19	502.63	522.415	542.2
20	542.63	567.915	593.2
21	593.63	624.915	656.2
22	656.63	696.915	737.2
23	737.63	787.915	838.2
24	838.63	901.915	965.2
25	965.63	1045.915	1126.2
26	1126.63	1227.415	1328.2
27	1328.63	1455.915	1583.2
28	1583.63	1744.415	1905.2
29	1905.63	2108.415	2311.2
30	2311.63	2566.915	2822.2
31	2822.63	3145.415	3468.2
32	3468.63	3864.415	4260.2
33	4260.63	4744.415	5228.2
34	5228.63	5820.915	6413.2
35	6413.63	7139.415	7865.2
36	7865.63	8753.415	9641.2
37	9641.63	10731.42	11821.2
38	11821.63	13156.42	14491.2

4 Data processing

The processing and the subsequent inversion of the TEMPEST and SkyTEM data was carried out using the Aarhus Workbench processing and inversion software (Auken et al. 2015). The processing procedure applied to the two datasets differed due to the nature of the provided raw data. The raw SkyTEM data was supplied by the contractor as .skb files and these along with a .geo file containing system specifications were imported into the Aarhus Workbench. The TEMPEST data on the other hand were supplied as a Geosoft database and the data was exported to a XYZ file for import into the Aarhus Workbench.

4.1 Processing of SkyTEM data

The following workflow was employed for the data processing of the acquired SkyTEM AEM data:

1. Import raw (.skb files) data to Workbench using contractor supplied line files and .geo file with system specifications such as waveform, channels, turns, filters etc.
2. Divide data into "processing nodes" according to flights or dates of acquisition.
3. For each "processing node" undertake:

   - Automatic processing of GPS position, tilt and altitude data of the transmitter frame;
   - Manual processing of altitude;
   - Apply topographic data set from external file;
   - Automatic processing of Low and High Moment response data (this includes averaging of the raw LM and HM moment data through filtering);
   - Manual editing of the automatically processed data to remove any cultural and late time noise which the automatic filter settings did not account for.

This workflow, and its implementation, was aimed at preparing the data for the full non-linear inversion step that followed (see Section 5).

4.1.1 PROCESSING OF GPS AND TRANSMITTER FRAME TILT DATA

The positions of the transmitter frame during survey acquisition were measured with two GPS receivers (GPS1 and GPS2). See acquisition and processing report for details of their positions on the transmitter frame (SkyTEM 2016). Both GPS1 and GPS2 record data during survey acquisition. Post-acquisition, differentially corrected positions can be obtained in conjunction with data from a ground base station. GPS2 uses the OMNISTAR high precision real time correction service, where differential corrections are received in real time. Therefore GPS2 data are used as the primary navigation data source for the survey.

The automatic processing of the GPS positions in Aarhus Workbench entails filtering and averaging of the data. GPS data positions are necessary for each individual sounding in order to use the derived dB/dt data. Tilt meters mounted on the front of the transmitter frame measure its attitude during data acquisition. Frame pitch and roll are recorded, and the resulting data are then filtered and averaged using a median filter.

4.1.2 PROCESSING OF THE ALTITUDE OF THE TRANSMITTER FRAME

The processing of the raw altitudes from the two laser altimeters fitted on the SkyTEM transmitter frame includes an automatic filtering and averaging process. A subsequent manual editing is often required to remove outliers, reflections not originating from the ground surface, and to correct the altitude for areas where the automatic filter applied to the data has been ineffective. During this processing the altitude data are also adjusted for the altimeter's deviation from a horizontal position.

Figure 6 shows how the recorded altitudes from the two altimeters can vary and how the processed altitude disregards laser reflections caused by other objects than the ground such as trees. The processed altitude was used as input into the inversion of the data.

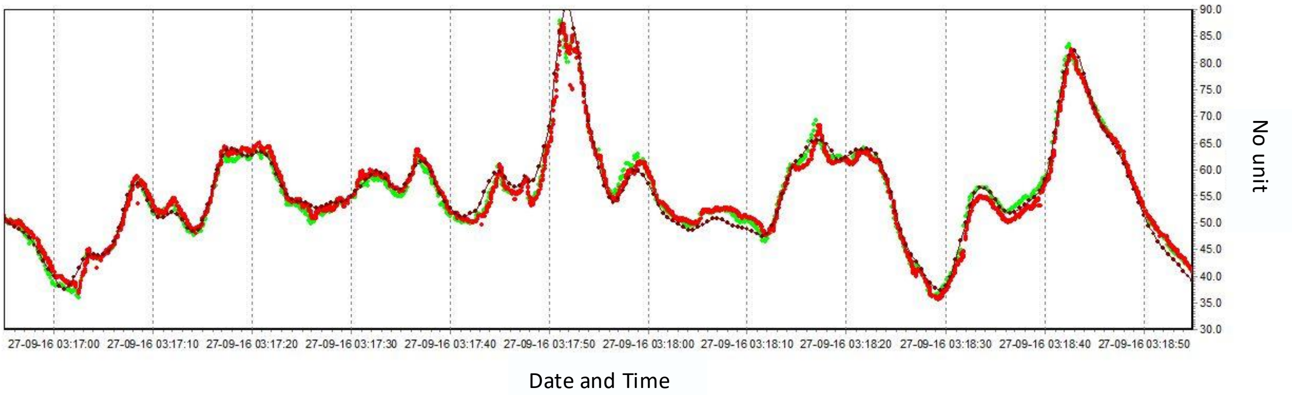

Figure 6. An example of the two altimeters (red and green) and the processed altitude (brown) for two minutes of data.

4.1.3 PROCESSING OF LOW AND HIGH MOMENT AMPLITUDE RESPONSE DATA

The automatic data processing applied to the Musgrave SkyTEM data set included the application of what is referred to as an averaging trapez filter. This helps remove late time noise and assists in the choice of the sounding distance (distance between soundings) of the averaged data. The width of the trapez filter was chosen so that it would average noise, while honouring the lateral structure seen in the amplitude response data. The filters have been kept as narrow as possible while still allowing the late times to be averaged adequately to improve the signal to noise ratio. For some parts of the survey area the noise levels are quite high, this is particularly the case for areas with limited cover. A consequence of a varying signal to noise ratio across the survey area, is that for the parts where the noise levels are very high the data is not useable as input into an inversion (Figures 7 and 8). In addition to the averaging trapez filters, automatic filters to remove late time noise are used cautiously (Figure 9). There are parts of the survey area where induced polarisation (IP) effects were seen in the SkyTEM data as negative decays at late times. The appearance of IP effects in airborne EM data sets has become increasingly apparent with significant improvements in system signal:noise and higher power (see for example, Smith 2016, and Viezzoli et al. 2017).

Induced polarization (IP) effects are not only evident as negative receiver voltage values, which in some cases are easy to detect, but they can also be present in these data as exceedingly fast decays, or erratic slopes/curvatures, without ever changing sign. Smith (2016) refers to such behaviour as 'shape reversals', where a high spatial frequency feature changes from a relative positive at early times to a relative negative at late times. In some cases, the most subtle IP effects will not become evident until modelling is attempted. Some shape reversals could be misinterpreted as three-dimensional (3D) effects, so care must be given to their study in data space, accompanied by an assessment of inversion outputs in the model space.

At the time of writing, the inversion codes employed here were unable to model AIP. Its presence can lead to significant artefacts in the resulting model if they are not first identified and removed. Therefore, for this study we filtered out the most obvious effects of IP, with soundings affected by IP manually identified and removed from the data set prior to inversion. Where possible, only late time channels were removed from the inversion. It needs to be stressed however, that AIP effects do not only affect “late times” (e.g., Smith 1989, Flis et al., 1989 and Viezzoli et al., 2016), but rather distort large portions of the entire transient. It is therefore virtually impossible to eliminate them totally from the measured data prior to inversion.

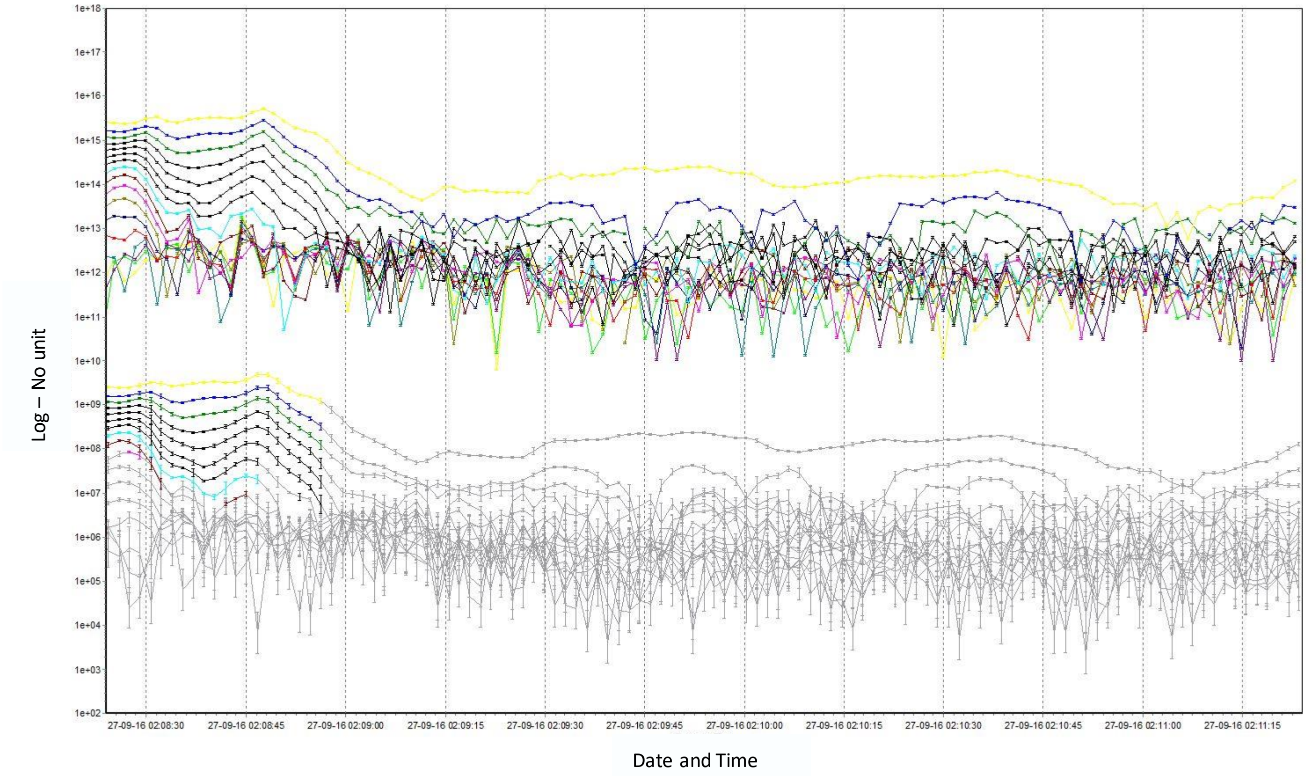

Figure 7. SkyTEM low moment raw amplitude response (top set of curves) and averaged amplitude response data (bottom set of curves) for part of a flight line. The greyed-out areas in the bottom panel are areas where the data is unusable due to high noise levels.

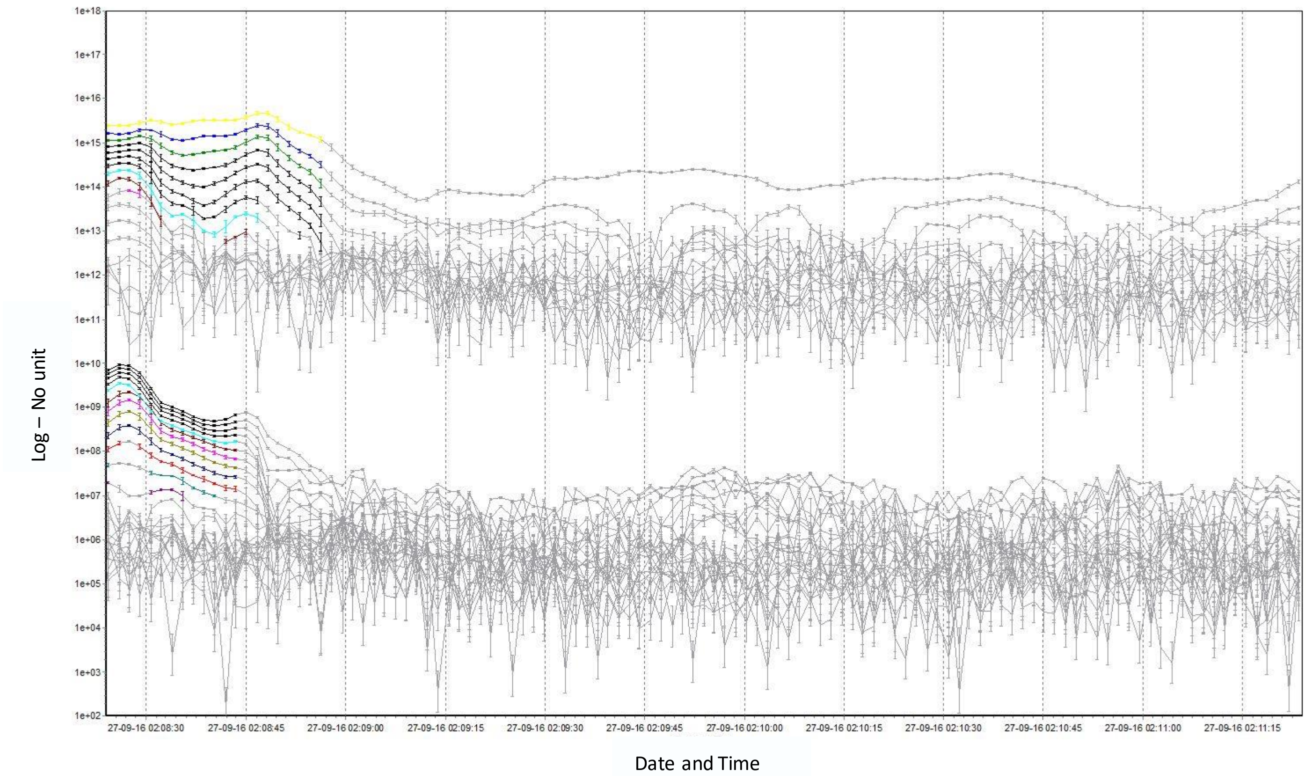

Figure 8. SkyTEM low moment averaged amplitude response (top set of curves) and high moment averaged amplitude response data (bottom set of curves) for part of a flight line. The greyed-out areas in both panels are areas where the data is unusable due to high noise levels.

During the manual processing the effect of the automatic filters is assessed and any remaining cultural and late time noise artefacts which the automatic filter settings did not account for are removed. Noise in the data can be caused by anthropogenic features such as powerlines or buildings. Figure 8 shows an example of the raw amplitude data for each gate for part of a flight line. Noise is assessed and then averaged (filtered), or removed where present. This is done for each flight line. In this example, low moment data for part of a line are displayed. Greyed out data points are data that have been removed during the processing – deemed to be affected by noise. The Low and High Moment raw amplitude data are also assessed independently. Once complete, the cleaned, processed data are then combined in a preliminary laterally constrained inversion (LCI) to assess if the manual processing was adequate, and to help choose the optimal inversion model parameters for application to the full data set.

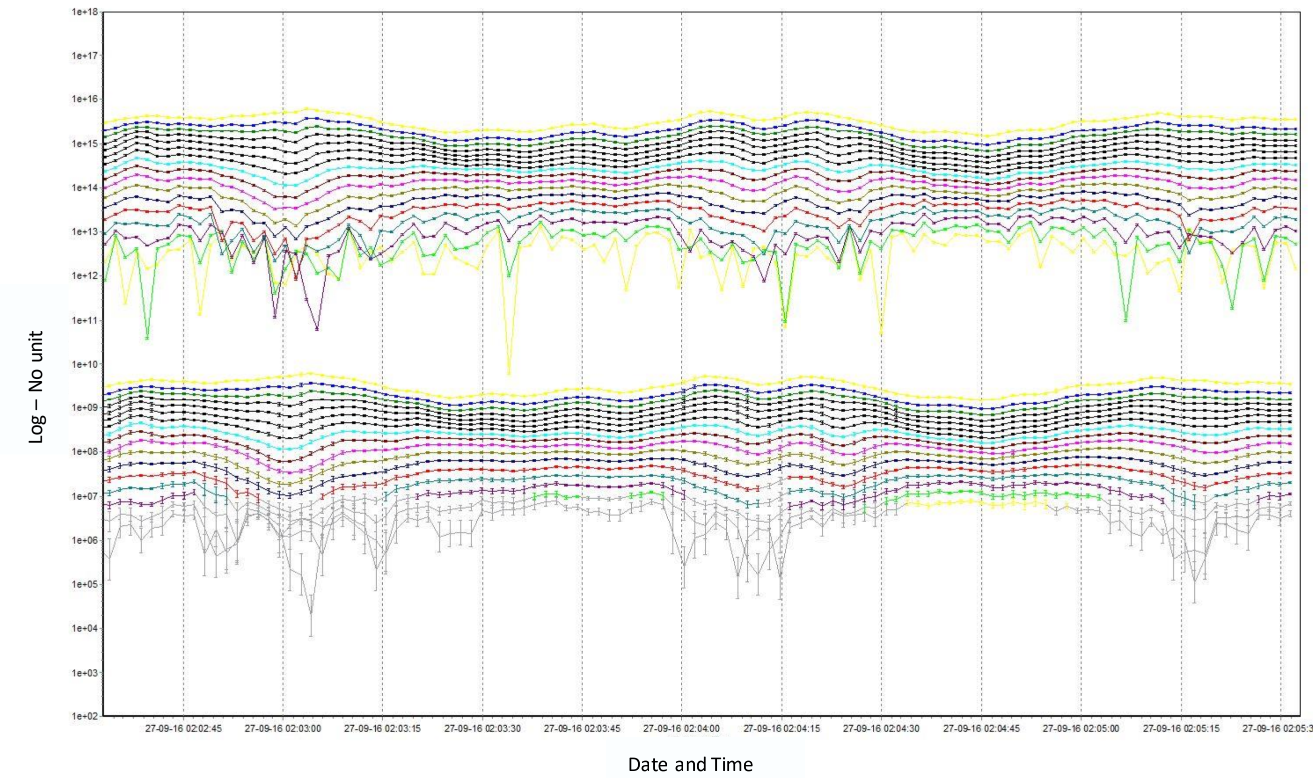

Figure 9. SkyTEM low moment raw amplitude response (top set of curves) and averaged amplitude response data (bottom set of curves) for part of a flight line. The greyed-out areas in the bottom panel are where late time noise has been removed either through the automatic filters or through a manual process.

4.2 Processing of TEMPEST data

The workflow for the processing of the TEMPEST data was similar to that employed for the SkyTEM data except for the GPS positions and transmitter height, as these have already been post-processed by the contractor (see logistics report: CGG 2016). There was no need for an extra averaging of the data as the supplied data already has been filtered. The workflow involved:

1. Import data to Workbench using contractor supplied data and a .geo file with system specifications such as waveform, channels, turns, filters, etc.
2. Divide data into “processing nodes” according to flights or dates of acquisition
3. For each “processing node” undertake:
   - Apply topographic data set from external file;
   - Automatic processing of X and Z component response data (to remove cultural and late time noise);
   - Manual editing of the automatically processed data to remove any cultural and late time noise which the automatic filter settings did not account for.

This workflow and its implementation was aimed at preparing the data for the full non-linear inversion step that followed (see Section 5).

4.2.1 PROCESSING OF X AND Z COMPONENT AMPLITUDE RESPONSE DATA

The Z and X component TEMPEST data, underwent an automatic filtering to remove negative values at late time caused by IP effects, as well as to remove general late time noise. The manual processing entailed a visual inspection of the automatic processing as well as additional removal of noise where needed (Figure 9).

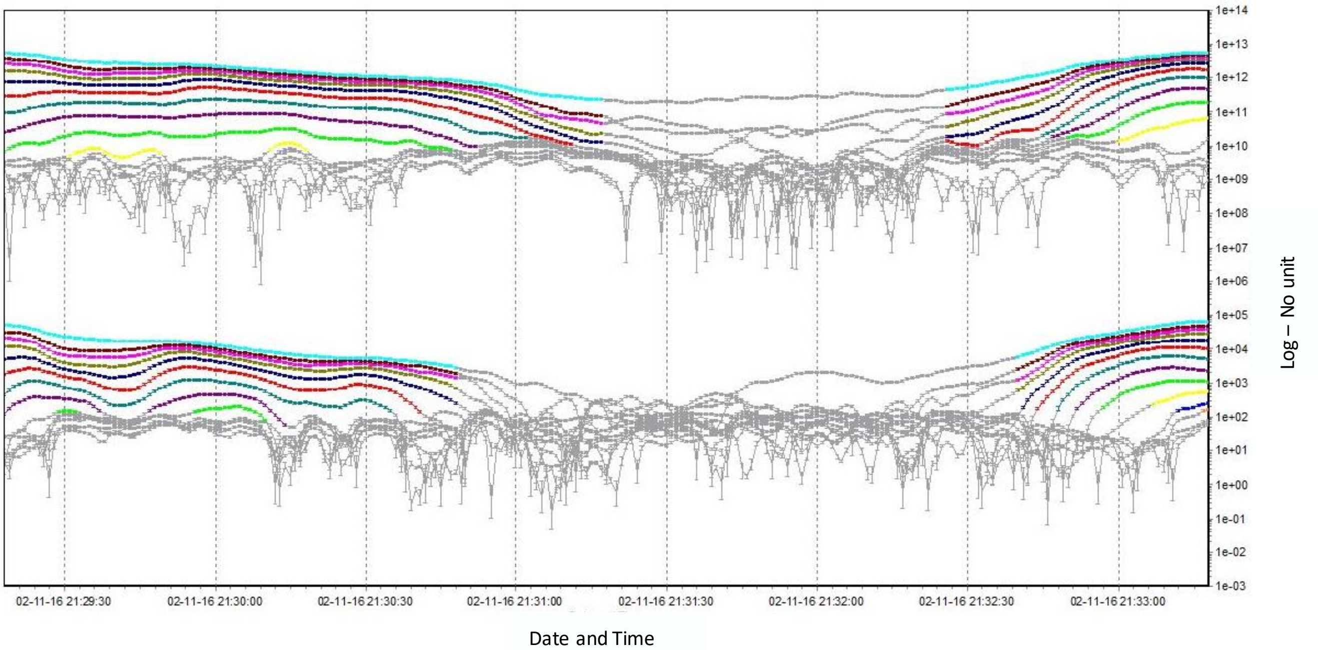

Figure 10. TEMPEST Z component amplitude response (top set of curves) and X component amplitude response data (bottom set of curves) for part of a flight line. The greyed-out areas are where noise has been removed either through automatic filtering or through a manual process.

4.3 Topographic data

In order to relate the conductivity-depth models derived through inversion to landscape geometry, a digital elevation model for the area was required. Each of the AEM surveys comes with their own topographical model obtained from the survey itself, but in order to relate the two datasets to the same reference topography, a 3 m orthophoto-derived DEM was chosen for this purpose (Figure 11).

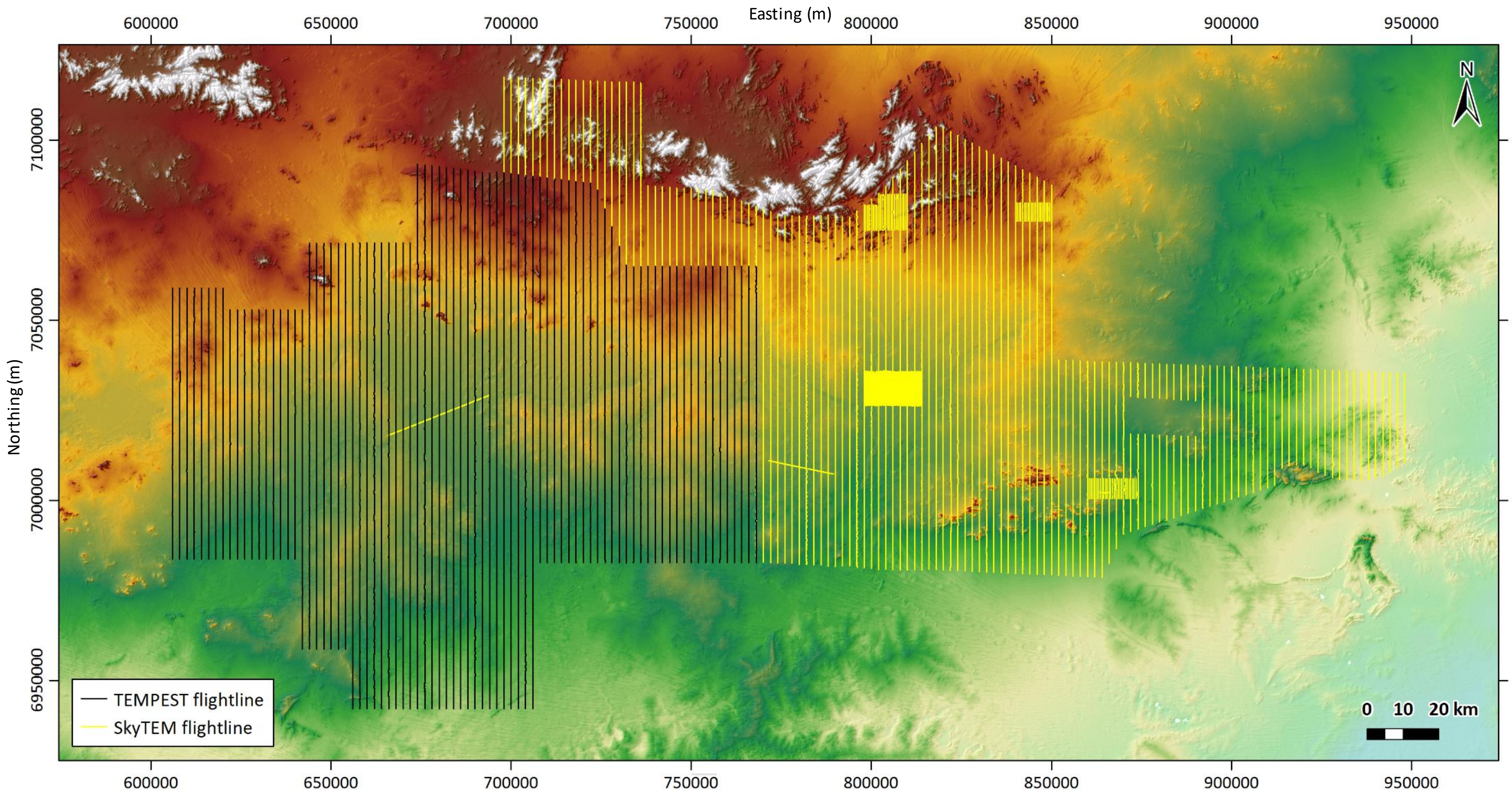

Figure 11. The flight lines for the TEMPEST (west) and SkyTEM (east) surveys overlain on the 3 m digital elevation model (DEM) supplied by Department of Mines and Energy.

5 Data inversion

5.1 Airborne electromagnetic data inversion

Measured AEM data can be imaged by gridding the raw window/time channels, where early times represent the near surface and late times greater depths. Although generally true, later times do not necessarily correspond to greater depth of penetration, and greater amplitude does not necessarily correspond with higher conductivity. These are therefore not a direct representation of a constant depth, but rather of a time slice of a response. While these might provide a quick overview of the spatial patterns of the data, they do not provide information about the conductivity distribution with depth. However, measured AEM responses can be converted from decay curves to information of conductivity variations with depth in the ground. This requires an inversion or transformation of the data.

Inversion of AEM data requires knowledge about the AEM system parameters, as an inversion basically entails an iterative process of minimising the misfit between the measured response, and a forward modelled response from a given earth model (consisting of a number of layers each with an associated conductivity). The parameters of the earth model is changed through an iterative process until an acceptable fit between the measured and modelled responses is achieved. The obtained conductivity-depth model can then be perceived to be a reasonable representation of a possible model. The inversion of AEM data is, however, a non-unique problem (i.e. several models are able to fit the data within the acceptable range). Consequently, models should be verified using independent information such as that can obtained from drill-holes. Inverted conductivity depth models along flight lines can be stitched together to form two-dimensional (2D) sections, and across lines to form spatial conductivity-depth slices.

Airborne electromagnetic (AEM) data acquired for exploration or environmental applications are commonly modelled using algorithms such as approximate transforms (Macnae et al. 1998; Christensen 2002) or Layered Earth Inversions (LEIs) that assume a 1D earth (Sattel 1998, 2005; Farquharson and Oldenburg 1998; Chen and Raiche 1998; Lane et al. 2004; Auken et al. 2005, 2015). Presently, the application and relevance of full 2.5 or 3D inversion of AEM data remains undetermined. In many respects it may be unrealistic and unnecessary, particularly for hydrogeological investigations in many Australian basins, where it is reasonable to assume that the subsurface can be represented as a series of horizontal layers. The 1D model assumption is also legitimate in sub-horizontal, layered sedimentary areas where it produces results that are only slightly distorted by 2D or 3D effects which may be induced by faults, fractures, or other geological phenomena (Newman et al. 1987; Sengpiel and Siemon 2000; Auken et al. 2005).

The geology of the Musgrave Province comprises Mezo-Proterozoic crystalline basement which in places outcrops as isolated hills and ranges, but other areas are covered by regolith. Groundwater is present in weathered and fractured basement sections, in buried palaeovalleys in calcretes and sediments consisting of alluvial, fluvial and Aeolian deposits (Watt and Berens 2011). A deep palaeovalley systems throughout the area are known to be present from limited drilling. The presence of wide palaeovalleys and what are likely to be sub-horizontal layers of sediments characterising much of the cover, it is reasonable to assume that the 1D assumption will be applicable in this setting, except in places where abrupt transitions in conductivity occur. In such instances, for example where regolith abuts against outcrop, it is possible that artefacts will be present in the inversion outputs. The inversion scheme used in the Aarhus Workbench software uses the full nonlinear inversion algorithm AarhusInv (Auken et al. 2015). This algorithm inverts soundings for a set of 1D models connected through constraints. The inversion requires a data file as well as a model input definition file containing information on starting model, regularisation constraints as well as any prior information. Both lateral and spatial constraints were employed in the inversion of the two regional data sets, with the spatially constrained inversion initially restricted to the processing of the closer spaced subsets of the SkyTEM data adjacent to the communities.

5.2 Inversion model

The Musgrave AEM surveys were inverted using a smooth layer model. This type of model typically consists of 15–30 layers with fixed thicknesses, often increasing with depth. The amount the conductivity of one layer can vary to the next is defined by a vertical constraint. The large number of layers and the gradual change in conductivity in this type of model makes the resulting conductivity models appear continuous. This in turn can make it difficult to pick layer boundaries as these may appear rather diffuse.

For the purposes of this study, a 30-layer model was used for the inversion of both the TEMPEST and the SkyTEM datasets. The first layer thickness was chosen to be 3 m with logarithmically increasing thicknesses to a depth of 300 m which is the depth of the last layer boundary. The starting model was a homogenous half space with an auto calculated conductivity, which is calculated as the mean of the apparent resistivity for each sounding. The regularisation constraints (smoothness constraints) were set to a vertical constraint of 3, a value which allows some vertical structure, without introducing artefacts caused by overfitting the data. The horizontal constraint was set to 1.8 for all layer intervals.

5.3 Laterally constrained inversion (LCI)

Both the regional SkyTEM and TEMPEST datasets were inverted using the laterally constrained inversion (LCI) methodology (Auken and Christiansen 2004; Auken et al. 2005). The spatial constraints, which are defined for adjacent soundings, allow prior information (e.g. the expected geological variability of the area) to migrate along the flight lines (Figure 12). The use of constraints along lines enhances the connection of layer parameters between adjacent soundings. In the context of the Musgrave Province this approach encourages the definition of laterally continuous conductive layers which is an aid to target definition and geological interpretation.

The inversion for the SkyTEM data solved for Z-component data as well as the transmitter height using the one model, whereas the inversion for the TEMPEST data solved for both the Z and X components along with transmitter height and the position and pitch of the receiver bird. This approach yields the maximum possible resolution of model parameters.

5.4

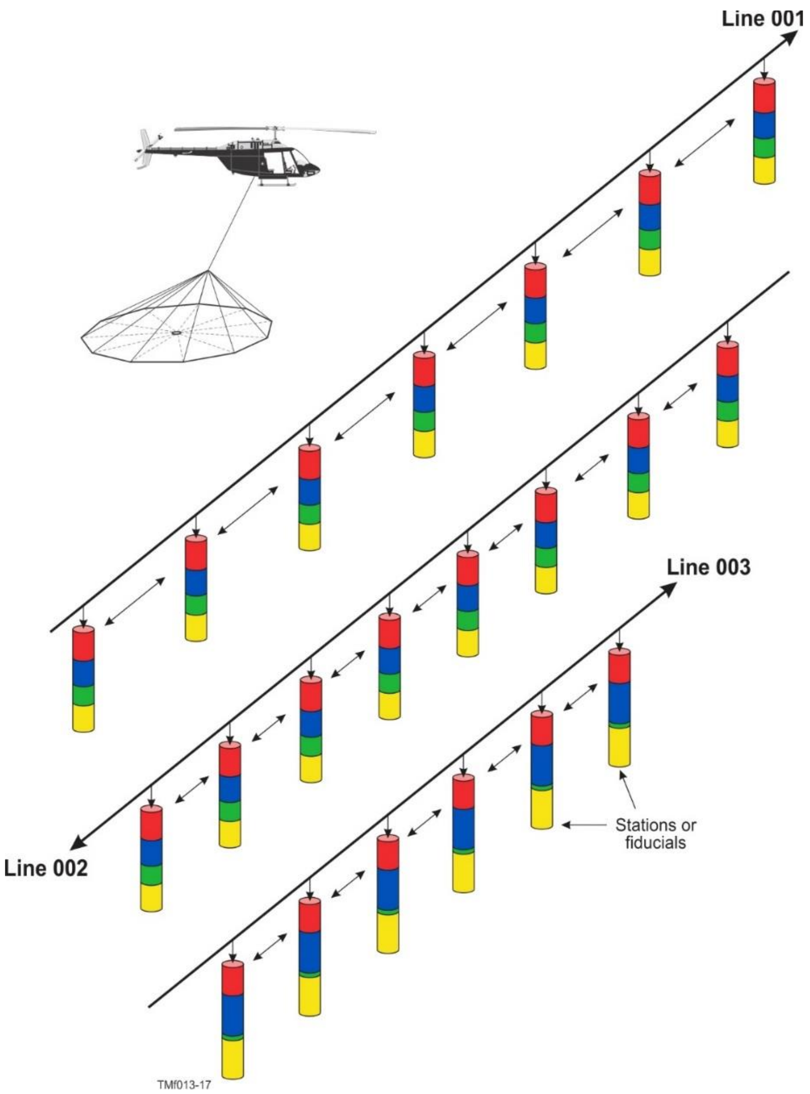

Figure 12. A diagrammatic representation describing the principle of laterally constrained inversion. Individual conductivity models of the subsurface derived from the inversion of individual soundings measured by the AEM system, are laterally correlated in the along-line direction to enhance the definition of laterally continuous conductive layers.

5.5 Spatially constrained inversion (SCI)

The SkyTEM^{312FAST} data for the infill areas (Figure 14) adjacent to the towns of Kaltjiti, Mimli, Yunyarinyi and Pukaja were inverted using the spatially constrained inversion (SCI) methodology described by (Viezzoli et al. 2009). The SCI is a quasi 3D inversion methodology, based on a 1D forward response, with 3D spatial constraints. The spatial constraints allow prior information (e.g. expected geological variability) to migrate along/through the entire dataset (Figure 13). This type of inversion uses constraints along lines and across lines, which means that layer parameters are connected between adjacent soundings.

The constraints for the SCI are set in a Delaunay triangulation, where the connection is made to the nearest neighbour. The advantage of using a spatially constrained inversion is seen in less striped inversion results as the geological information from one line to another is carried across. The output models balance the information present locally within the individual TEM soundings with the ones carried by the constraints, in this case from adjacent soundings. The SCI has a demonstrated applicability in semi-layered environments including those encountered in the palaeovalley sediment packages of the Musgrave province.

The inversion solved for both the Low and High Moment Z-component data as well as the transmitter height using the one model. This approach yields the maximum possible resolution of model parameters, as the Low Moment contains information from the near surface, and the High Moment information relating to the deeper part of the models.

5.6 Interval conductivities and conductivity depth sections

Conductivity-depth intervals or interval conductivities were generated from the inversion results of both the regional TEMPEST and the SkyTEM surveys, in 10 m intervals from surface to 200 m depth. Displaying inversion results as conductivity-depth images is a common way to visualise the spatial distribution of the conductivity within a survey area. In areas with large topographical variations it can be beneficial to display conductivities not only with depth but also as elevation intervals, accounting for variations caused by the topography.

Example interval conductivities for the two regional surveys are shown overlaid on a hydrogeological framework map (Figures 15-17), and a first vertical derivative (1VD) of airborne magnetic data map (Figures 18-20). The intervals were gridded using kriging with a cell size of 400 m.

Similar maps for each of the infill areas flown in the Eastern part of the Musgrave Province are shown in Figures 20-28.

Conductivity-depth sections have also been generated for each flight line through both regional surveys and for the infill areas. These have the Depth of Investigation (DOI) (see next section) appended to assist interpretation. An example of the nature of these sections is presented in Figure 29; in this example the results from the inversion of overlapping flight lines in the central part of the study area.

5.7 Depth of investigation

The presentation of conductivity models derived from AEM systems can be misleading if there is no attempt made to qualify the depth of investigation (DOI) of the measurement system. The depth of investigation is a complex quantity, being a function of the power, sensitivity and accuracy of the acquisition system, environmental noise levels (e.g. sferics -a broadband electromagnetic impulse that occurs as a result of natural atmospheric lightning discharges, and powerline sources), geologic complexity, the host conductivity and the target characteristics (e.g. a discrete object or an extensive layer, conductivity contrast to the surrounds) and the inversion procedure used (Christiansen and Auken 2012). To ensure that the observed variations in measured conductivity reflect changing ground conditions, rather than inversion or model dependent changes arising from the inversion process, an estimate of the depth of investigation is calculated and presented on the conductivity-depth sections. This information assists the interpreter, helping to quickly evaluate the results and their validity. The DOI provides a depth to which the model is the most reliable, and model information below the DOI should be used with caution.

The DOI determination used here is based on the cumulative sensitivity of the actual model output from the inversion (it includes the full system response and geometry) and is described in Christiansen and Auken (2012). The data noise and the number of data points are integrated into the calculation, which is based on the final inversion model output and a recalculated sensitivity (Jacobian) matrix. In general terms the more conductive the ground, the ability to resolve deeper variations in conductivity (or the depth to which the inverted model is reliable) decreases. In more resistive ground, the system is able to resolve those variations more reliably to greater depths. Modelled conductivities across the Musgrave Province study area result in a DOI that varies significantly (e.g. see Figure 29).

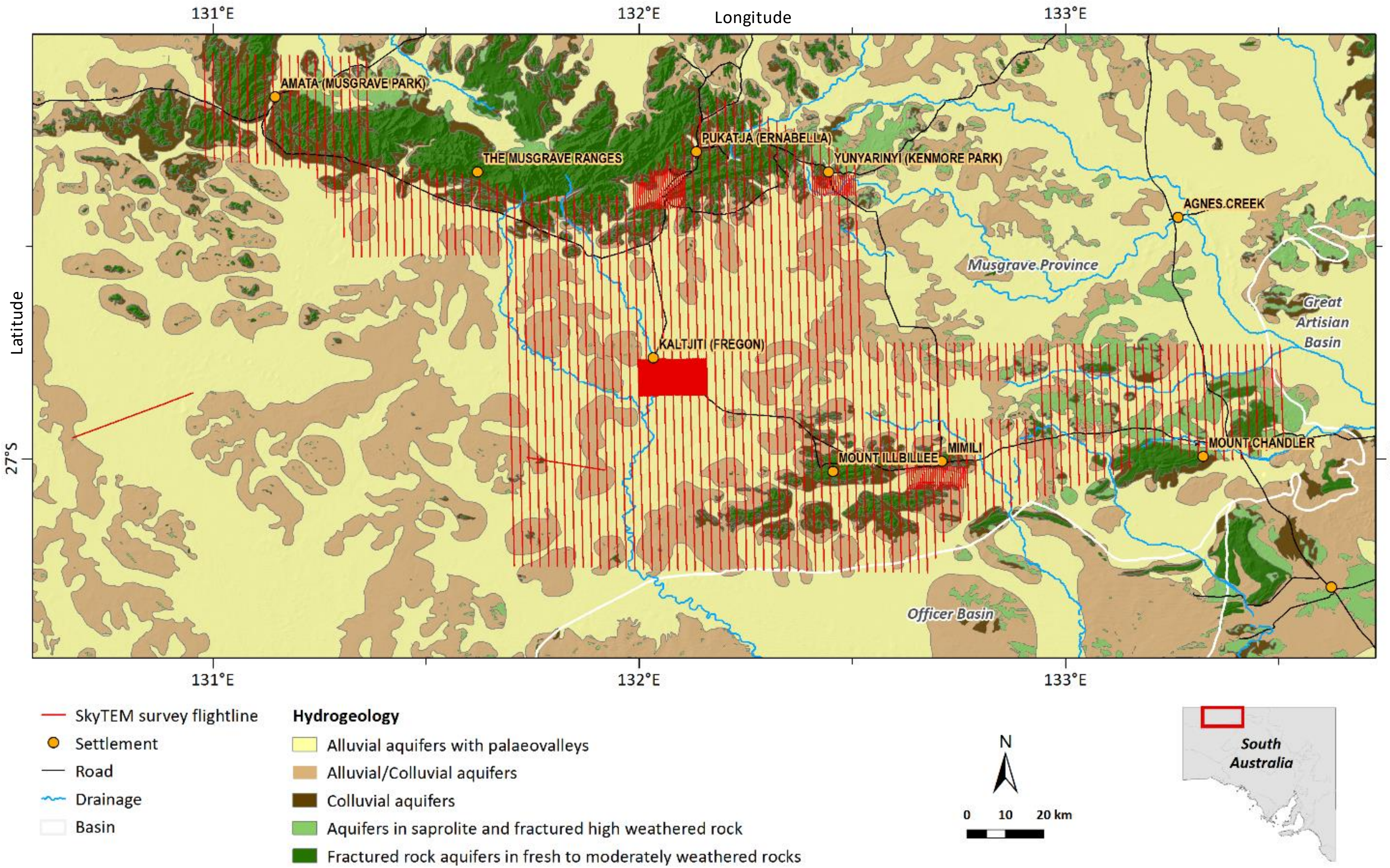

Figure 13. Flight line map for SkyTEM survey in the eastern Musgrave Province, showing the location of higher resolution survey areas (denser red lines) adjacent to Mimli in the south, Kaltjiti in the east, an area south west of Pukatja in the north and just south of Ymyarinyi in the north eastern part of the survey. Flight lines are overlain on hydrogeological framework map (Munday et al. 2013).

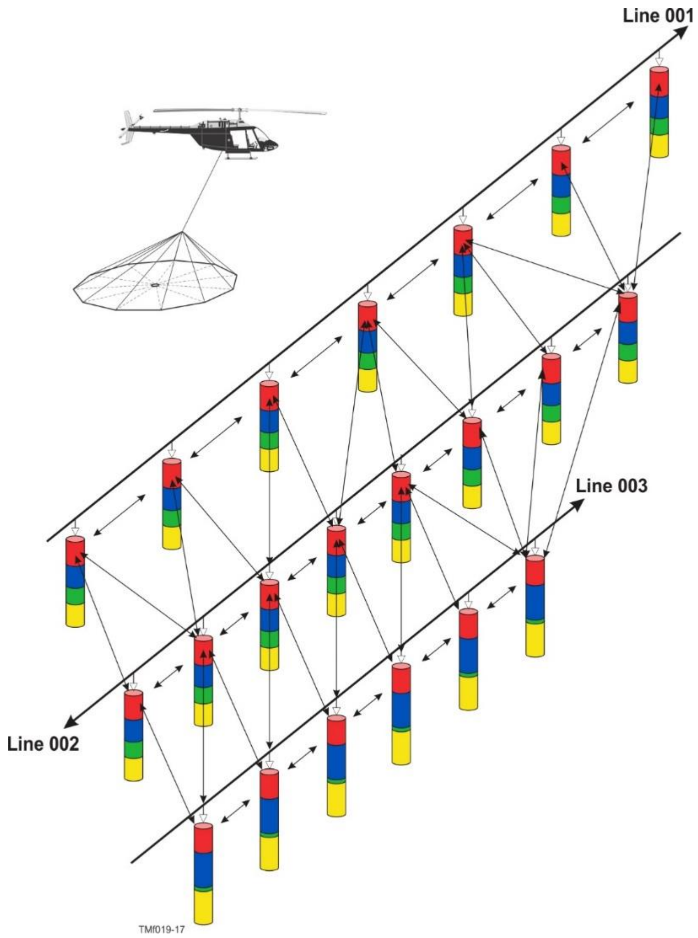

Figure 14. Schematic describing the process of allowing prior information to migrate along or through a series of soundings acquired by an AEM system when they are inverted using the Spatially Constrained Inversion procedure (SCI). In the case of the Musgrave subset areas, prior information is allowed to proceed from sounding to sounding along and across the flight lines.

5.8 Airborne induced polarization (IP)

In the analyses of the SkyTEM data over the Musgrave Province, induced polarization (IP) effects are evident in the data set and are most easily identified as negative receiver voltage values which in some cases are easy to detect. However, they can also be present in these data as exceedingly fast decays, or erratic slopes/curvatures, without ever changing sign. Smith (2016) refers to such behaviour as 'shape reversals', where a high spatial frequency feature changes from a relative positive at early times to a relative negative at late times. In some cases, the most subtle IP effects will not become evident until modelling is attempted.

We believe that similar effects are also present in the TEMPEST HM data set, but deconvolution of these data during pre-processing prevents their resolution. In the preliminary processing of the SkyTEM data, soundings affected by IP were manually identified and removed from the data set prior to inversion. Its presence can lead to significant artefacts in the resulting model if they are not first identified and removed. Where possible, only late time channels were removed from the inversion. It needs to be stressed however, that AIP effects do not only affect “late times” (e.g. Smith 1989; Flis et al. 1989; Viezzoli et al. 2016), but rather distort large portions of the entire transient. It is therefore virtually impossible to eliminate them totally from the measured data prior to inversion.

Further discussion of these issues, particularly as they relate to the regional AEM data sets acquired across the Musgrave Province, is presented in Soerensen and Munday (2018).

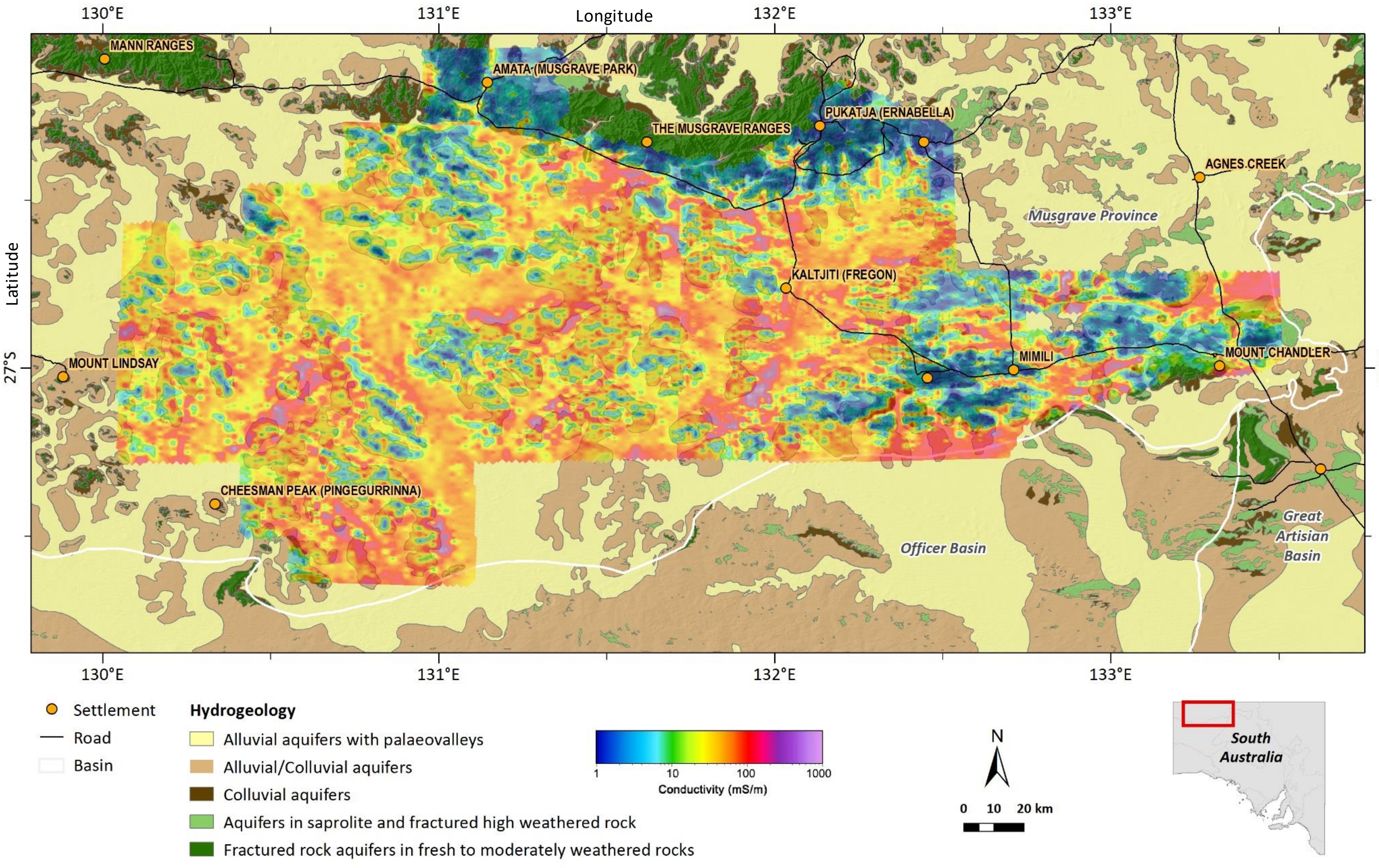

Figure 15. Airborne electromagnetic (AEM) inversion 10-20 m conductivity depth slice overlaid on a hydrogeological framework map (Munday et al. 2013).

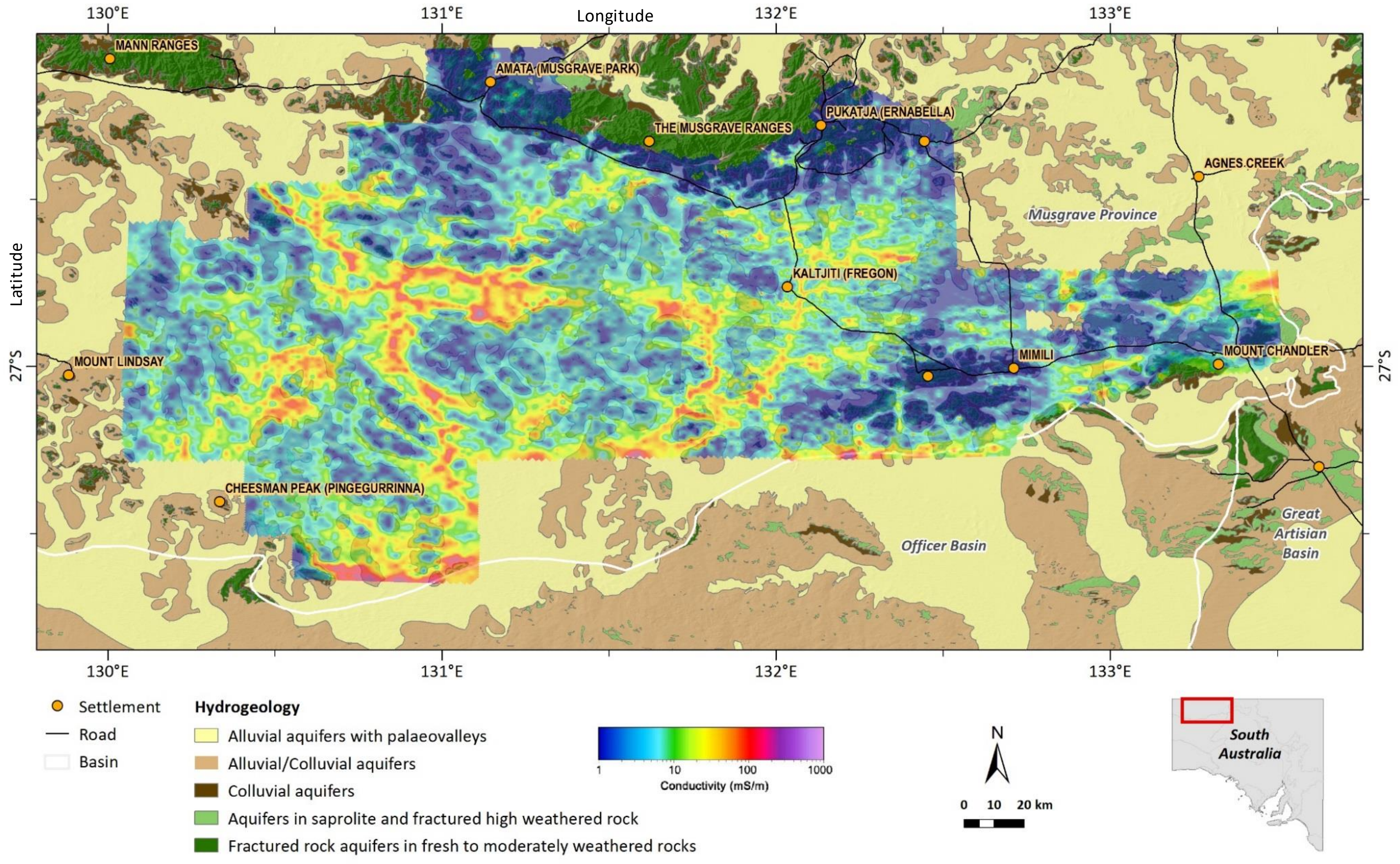

Figure 16. Airborne electromagnetic (AEM) inversion 50–60 m conductivity depth slice overlaid on a hydrogeological framework map (Munday et al. 2013).

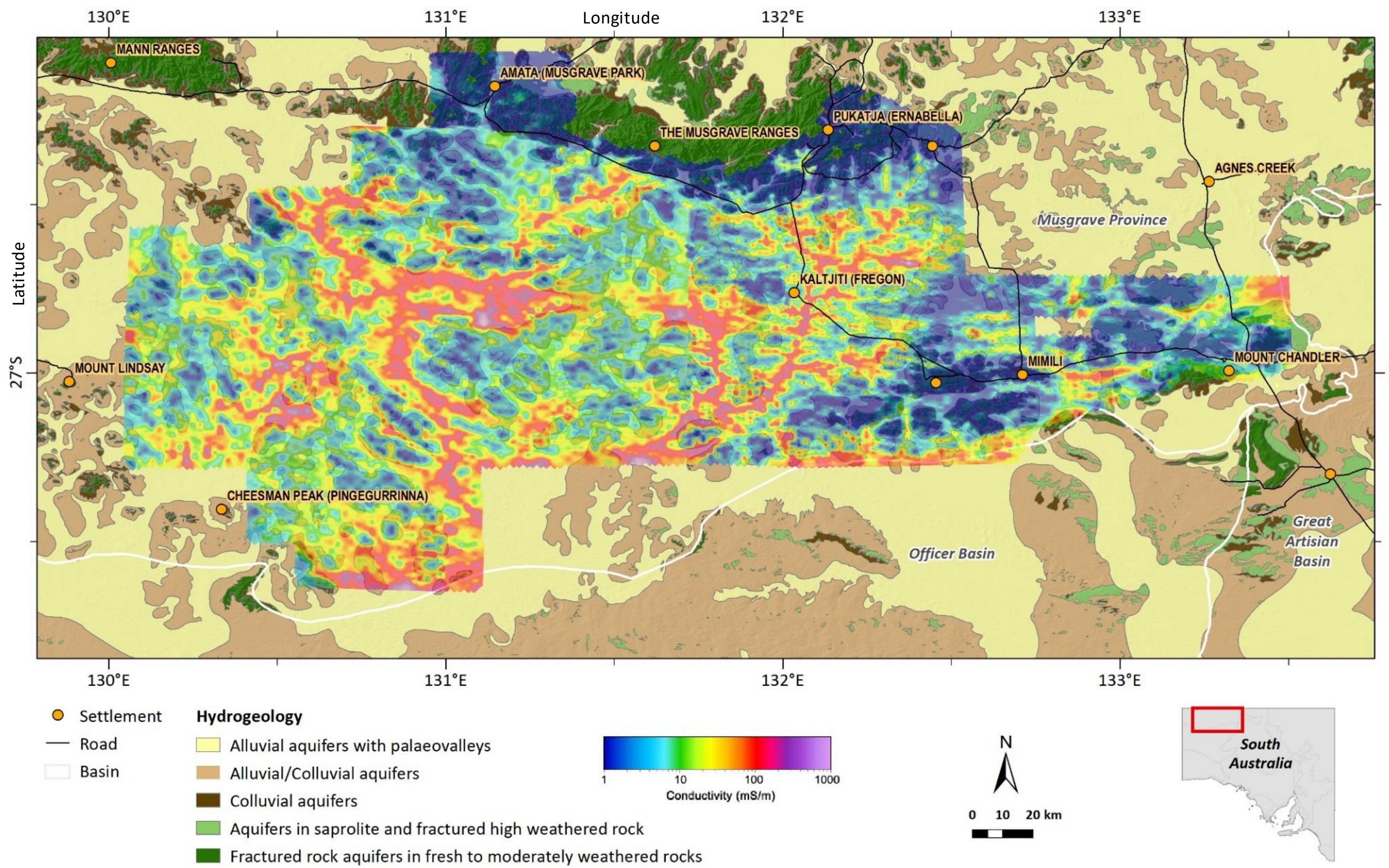

Figure 17. Airborne electromagnetic (AEM) inversion 90–100 m conductivity depth slice overlaid on a hydrogeological framework map (Munday et al. 2013).

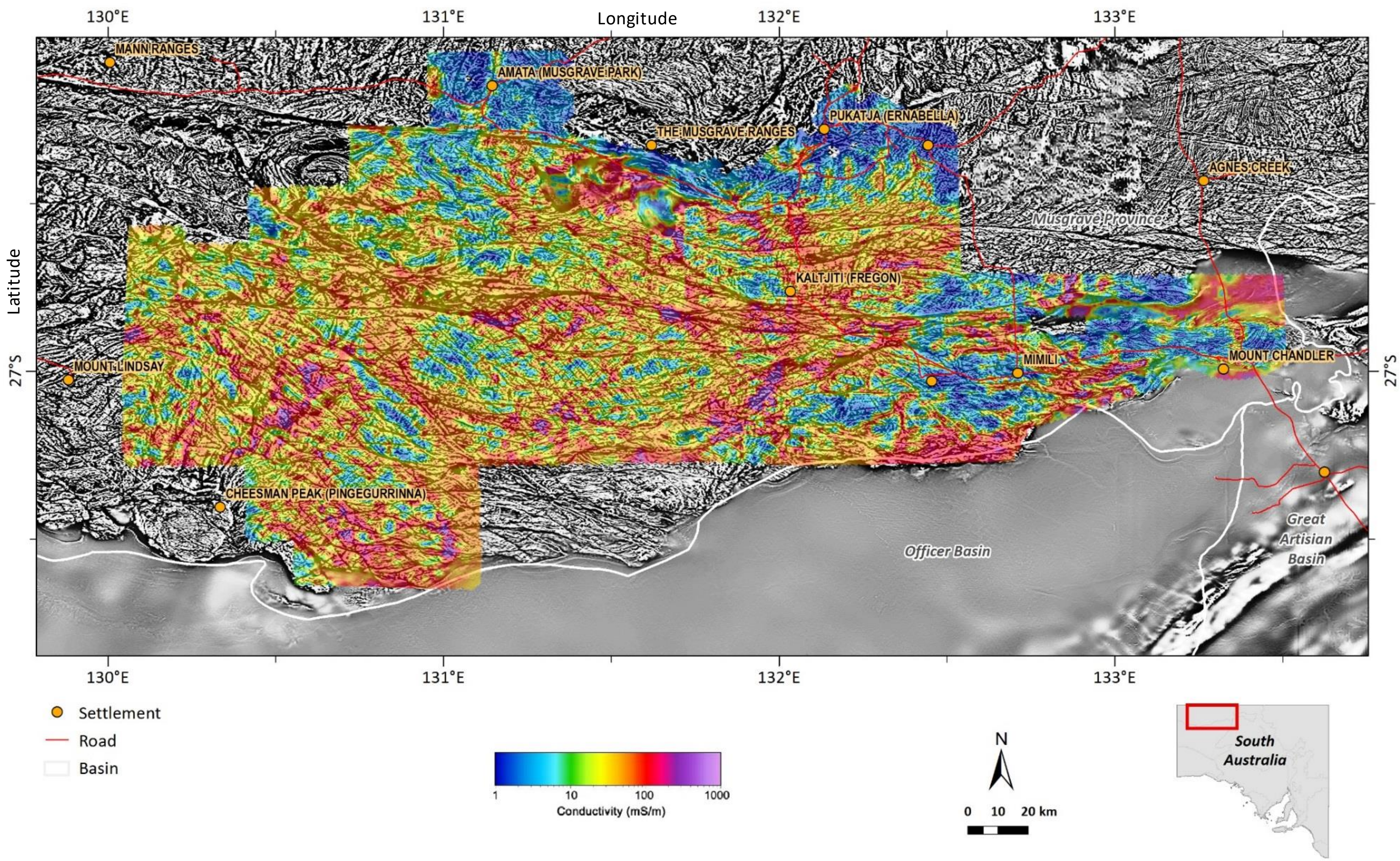

Figure 18. Airborne electromagnetic (AEM) inversion 10–20 m conductivity depth slice overlaid on a first vertical derivative (1VD) of the airborne magnetic data.

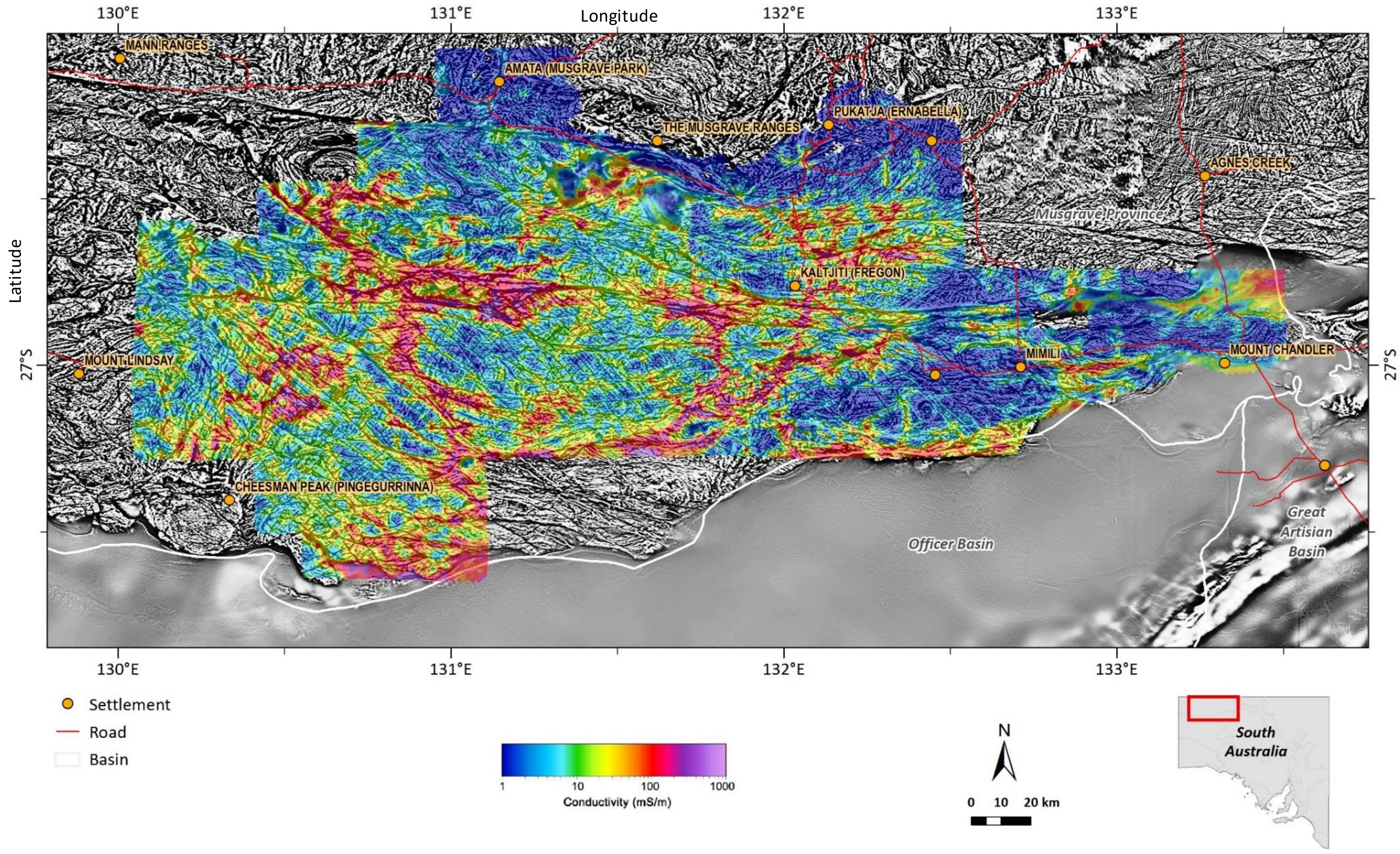

Figure 19. Airborne electromagnetic (AEM) inversion 50–60 m conductivity depth slice overlaid on a first vertical derivative (1VD) of the airborne magnetic data.

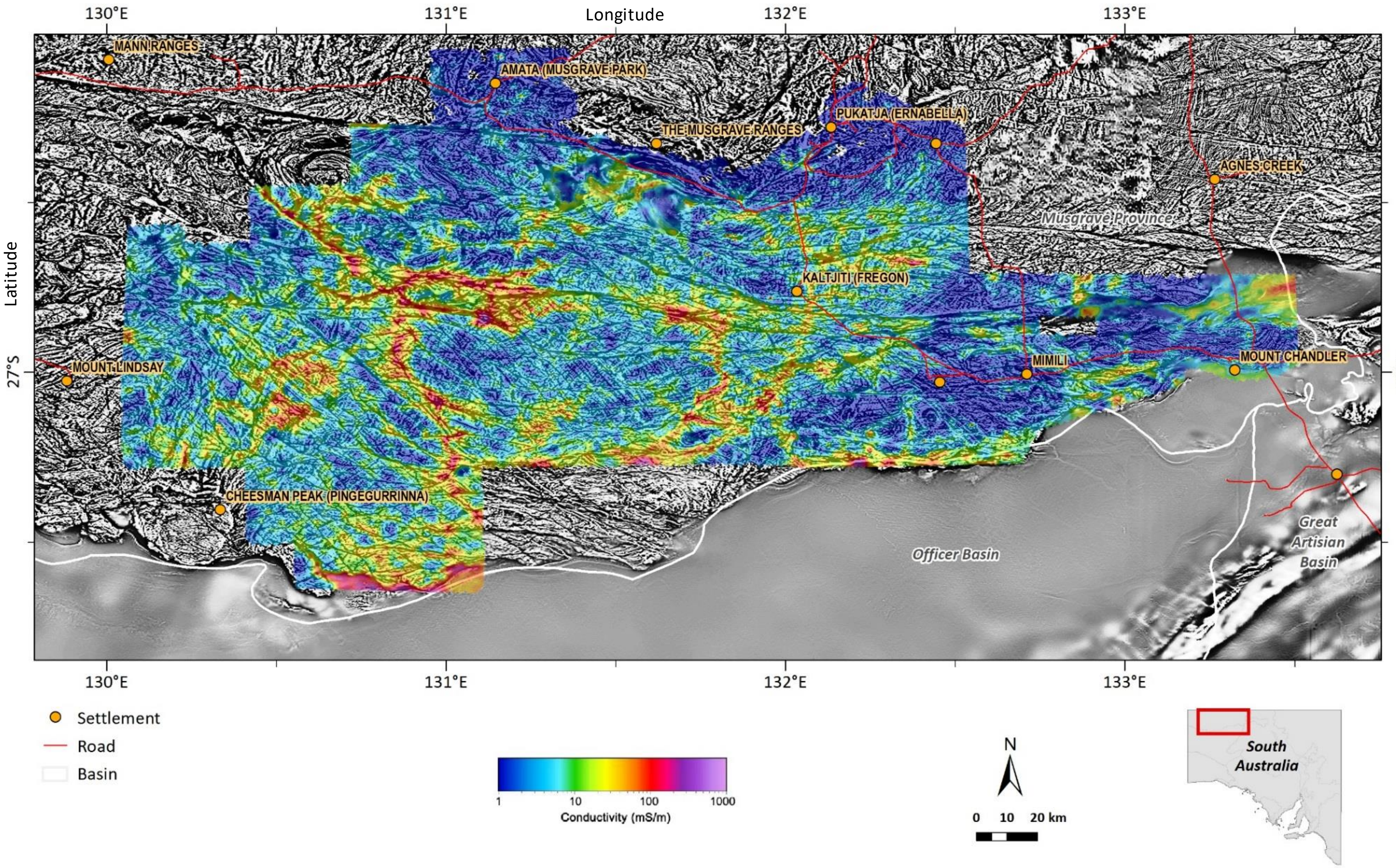

Figure 20. Airborne electromagnetic (AEM) inversion 90–100 m conductivity depth slice overlaid on a first vertical derivative (1VD) of the airborne magnetic data.

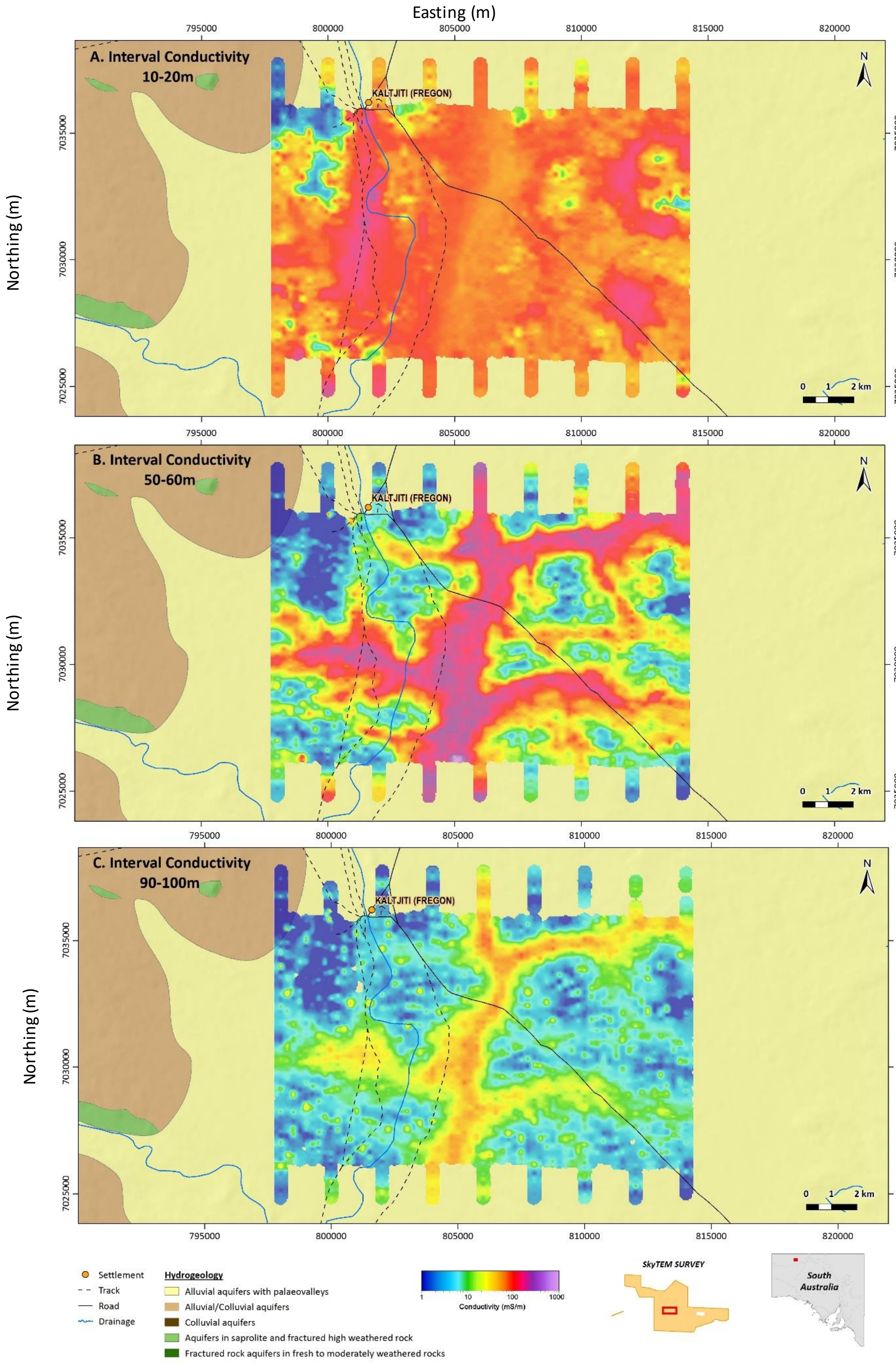

Figure 21. SkyTEM spatially constrained inversion (SCI) interval conductivities for the infill area south of Kaltjiti (Fregon). Intervals are overlain on hydrogeological framework map.

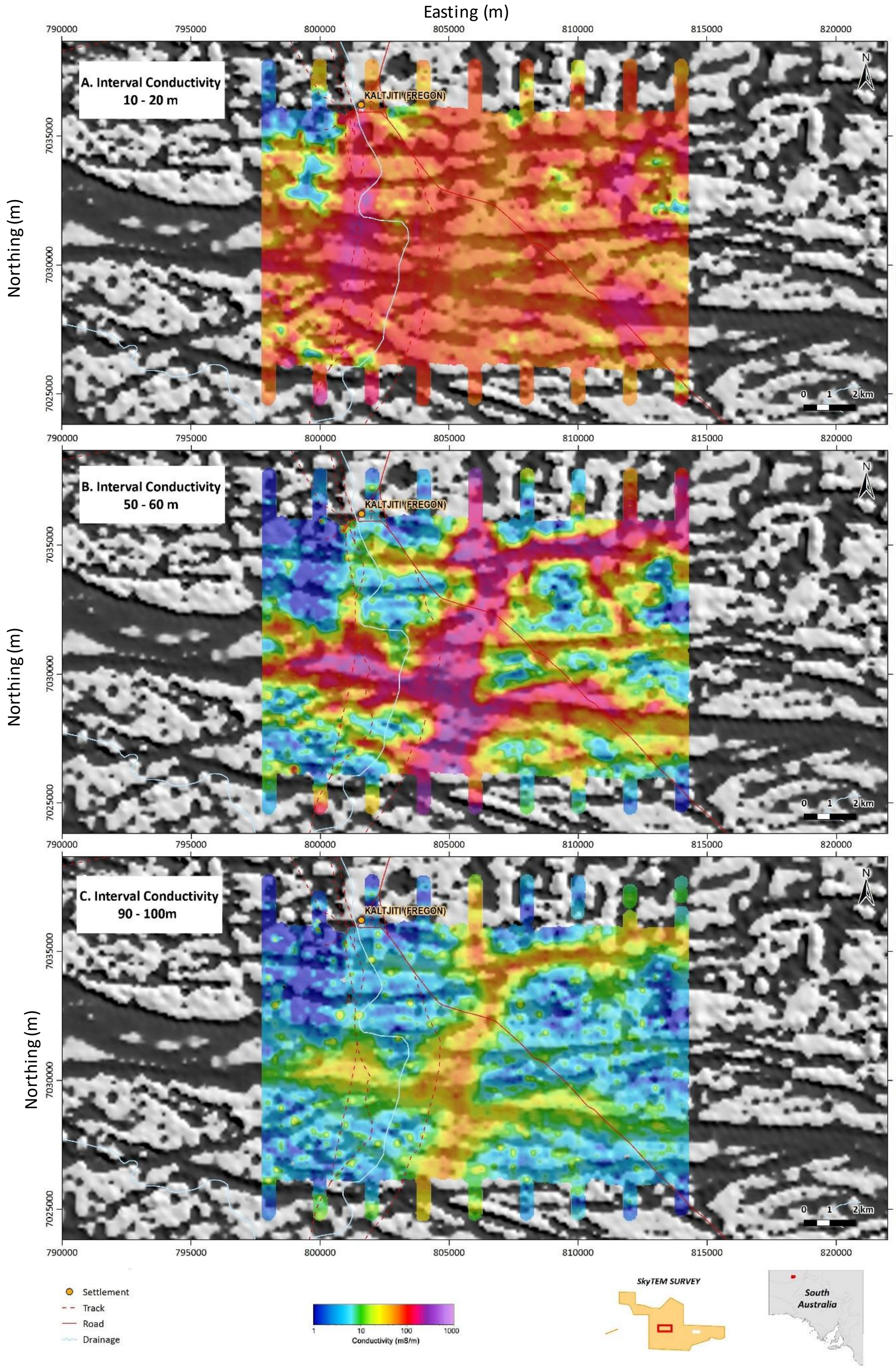

Figure 22. SkyTEM spatially constrained inversion (SCI) interval conductivities for the infill area south of Kaltjiti (Fregon). Intervals are overlain on first vertical derivative (1VD) of airborne magnetics greyscale image.

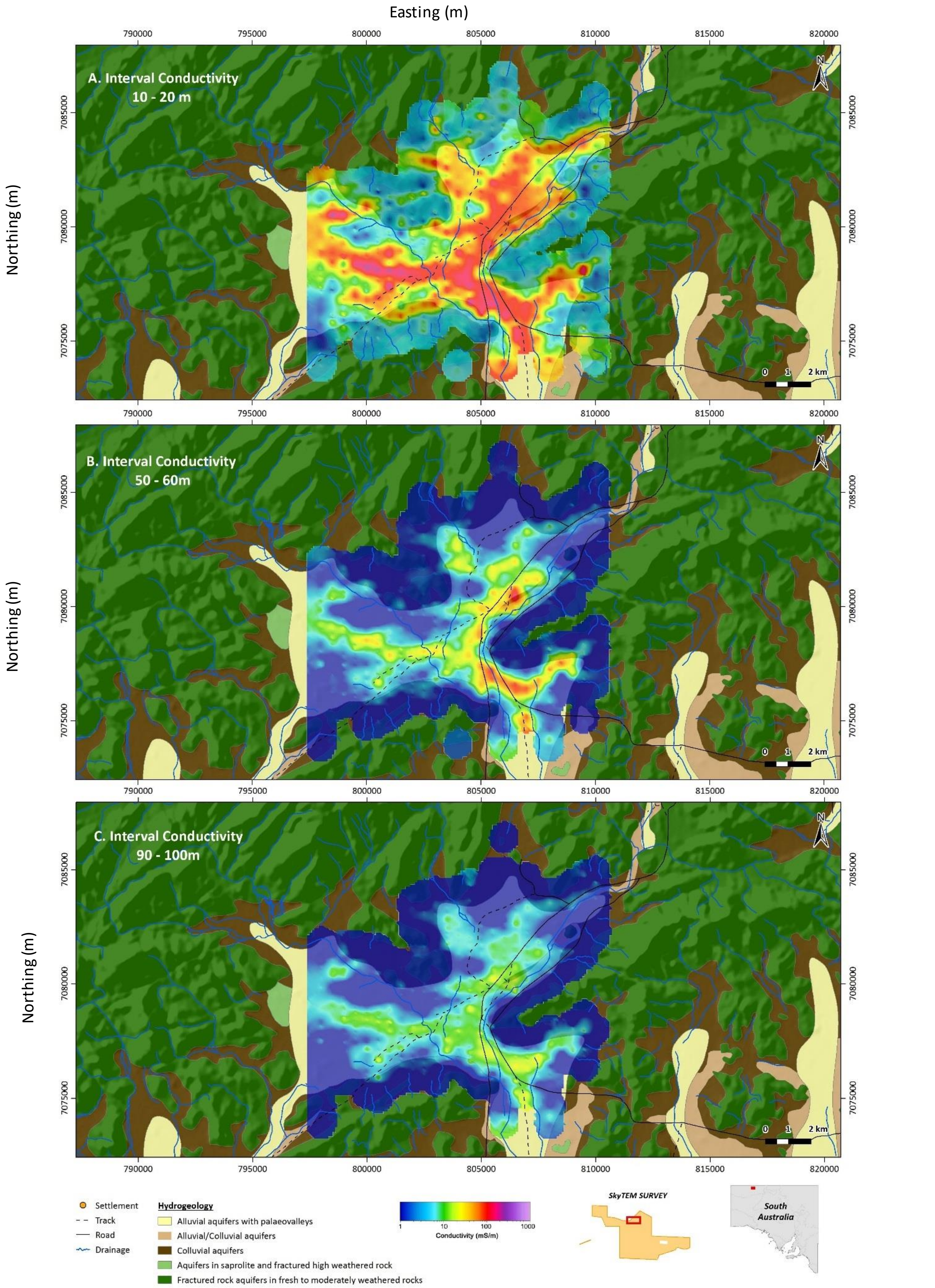

Figure 23. SkyTEM spatially constrained inversion (SCI) interval conductivities for the infill area south-east of Pukatja. Intervals are overlain on hydrogeological framework map.

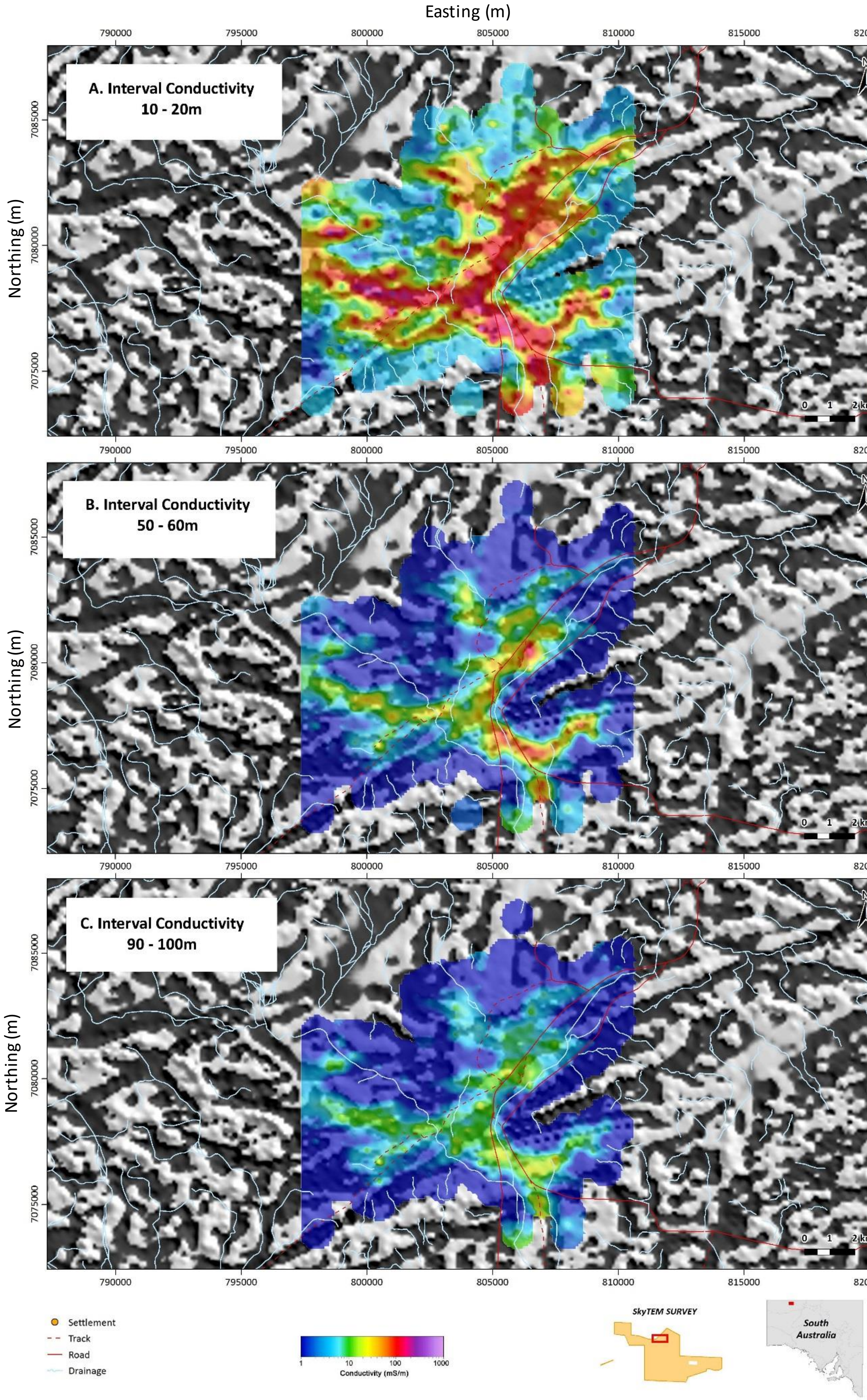

Figure 24. SkyTEM spatially constrained inversion (SCI) interval conductivities for the infill area south-east of Pukatja. Intervals are overlain on first vertical derivative (1VD) magnetic greyscale image.

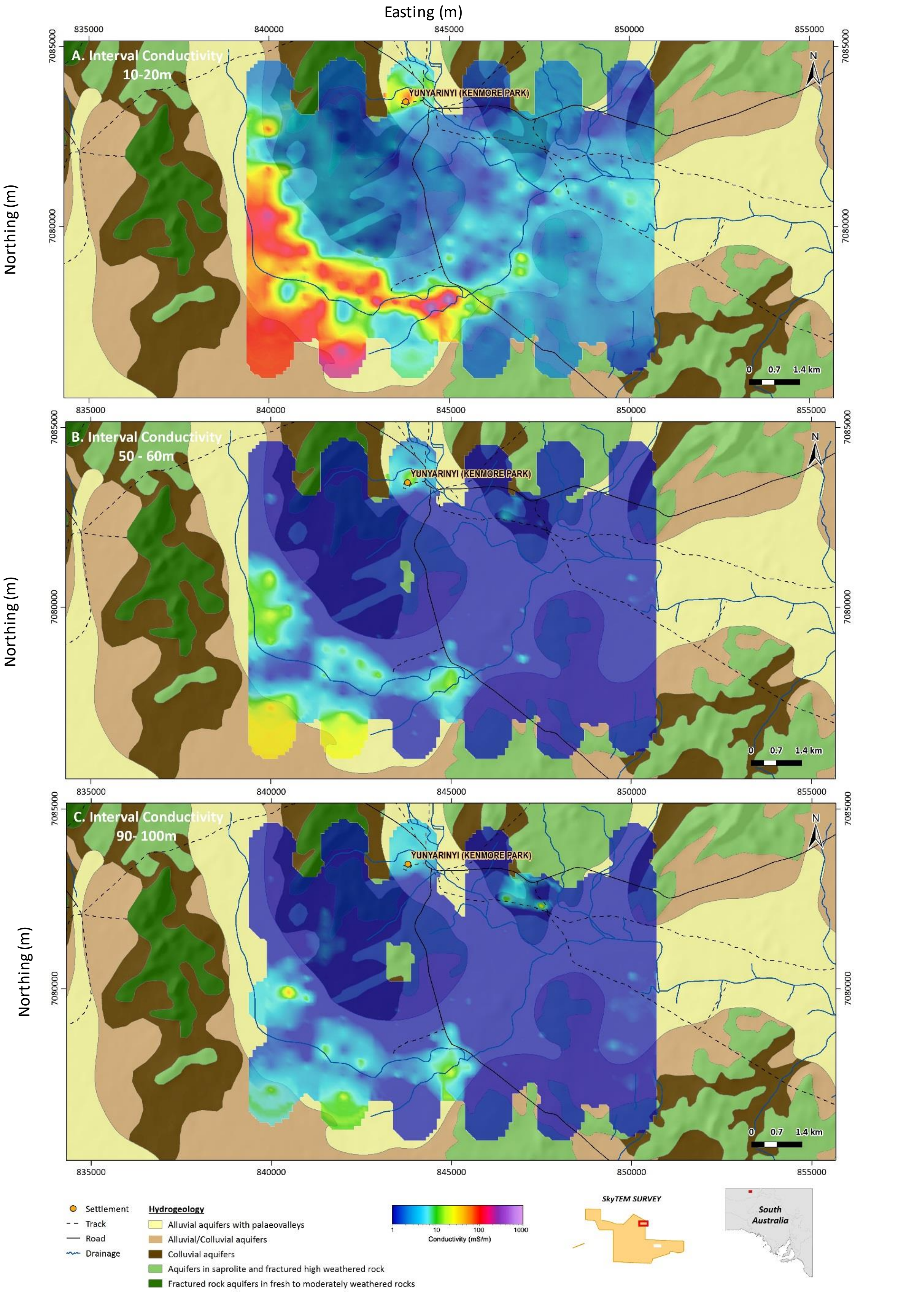

Figure 25. SkyTEM spatially constrained inversion (SCI) interval conductivities for the infill area south of Yunyarinyi. Intervals are overlain on hydrogeological framework map.

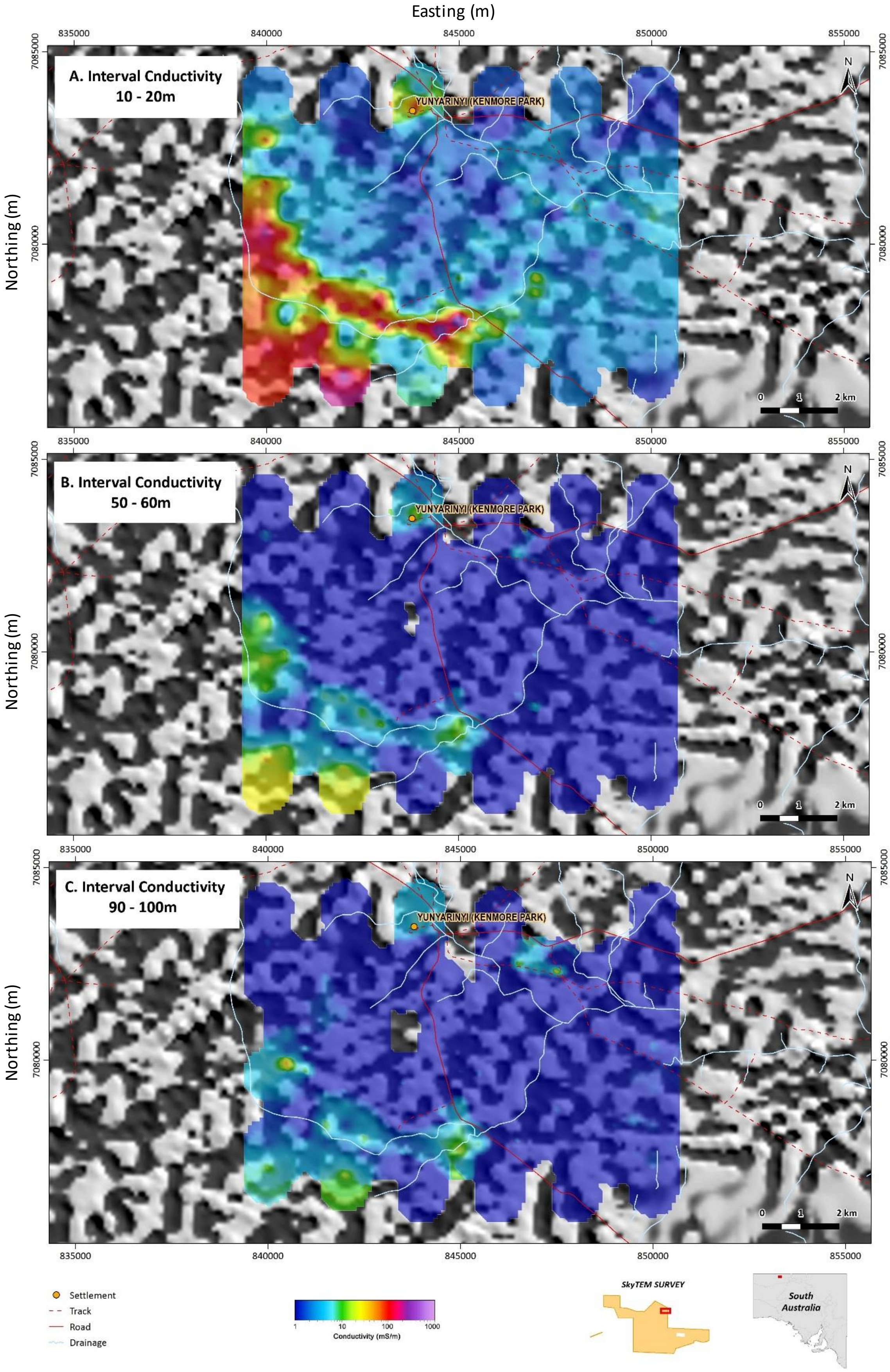

Figure 26. SkyTEM spatially constrained inversion (SCI) interval conductivities for the infill area south-east of Yunyarinyi. Intervals are overlain on first vertical derivative (1VD) magnetic greyscale image.

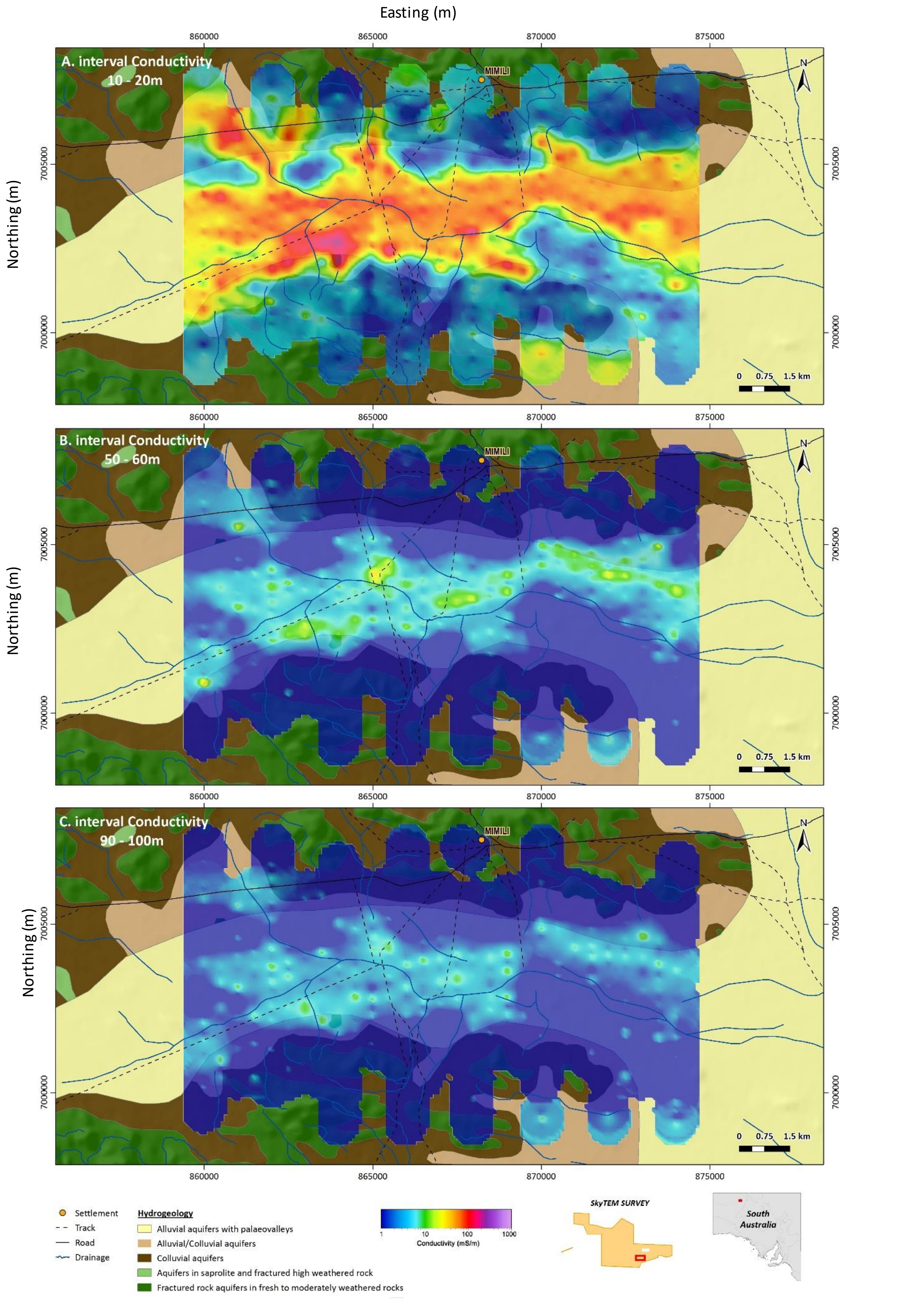

Figure 27. SkyTEM spatially constrained inversion (SCI) interval conductivities for the infill area south of Mimili. Intervals are overlain on hydrogeological framework map.

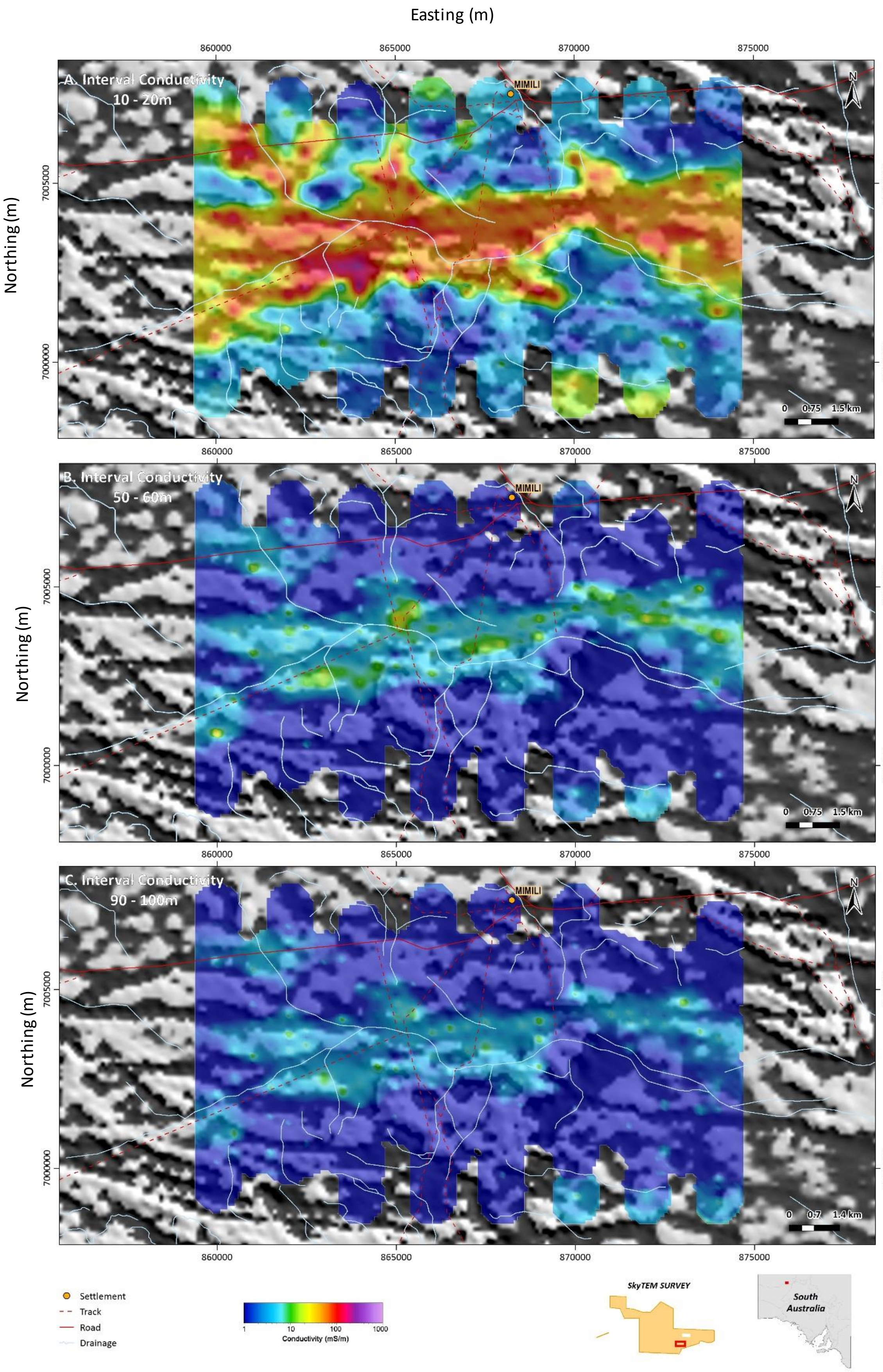

Figure 28. SkyTEM spatially constrained inversion (SCI) interval conductivities for the infill area south-east of Mimili. Intervals are overlain on first vertical derivative (1VD) magnetic greyscale image.

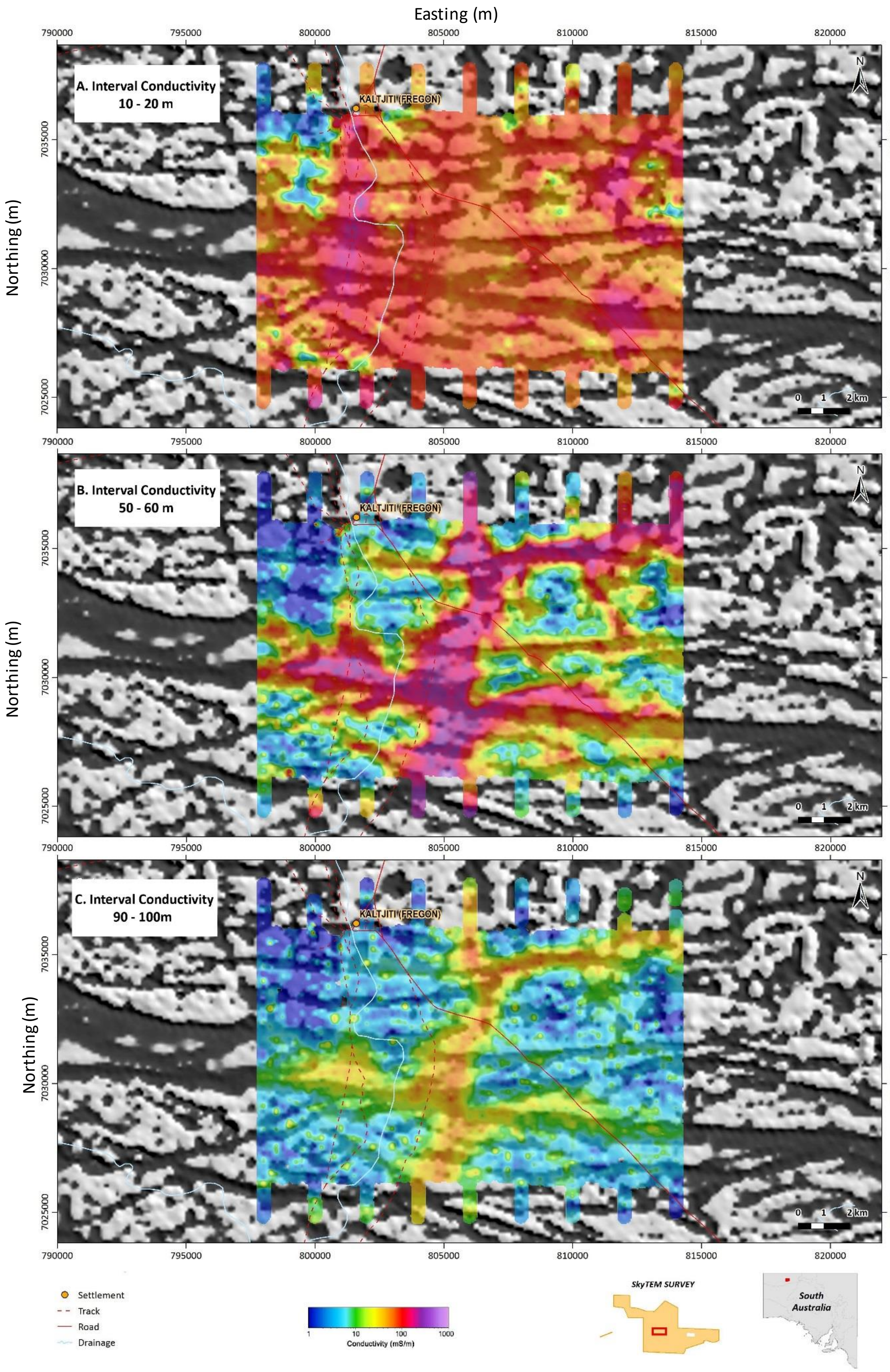

Figure 29. SkyTEM spatially constrained inversion (SCI) interval conductivities for the infill area south of Kaltjiti (Fregon). Intervals are overlain on first vertical derivative (1VD) of airborne magnetics greyscale image.

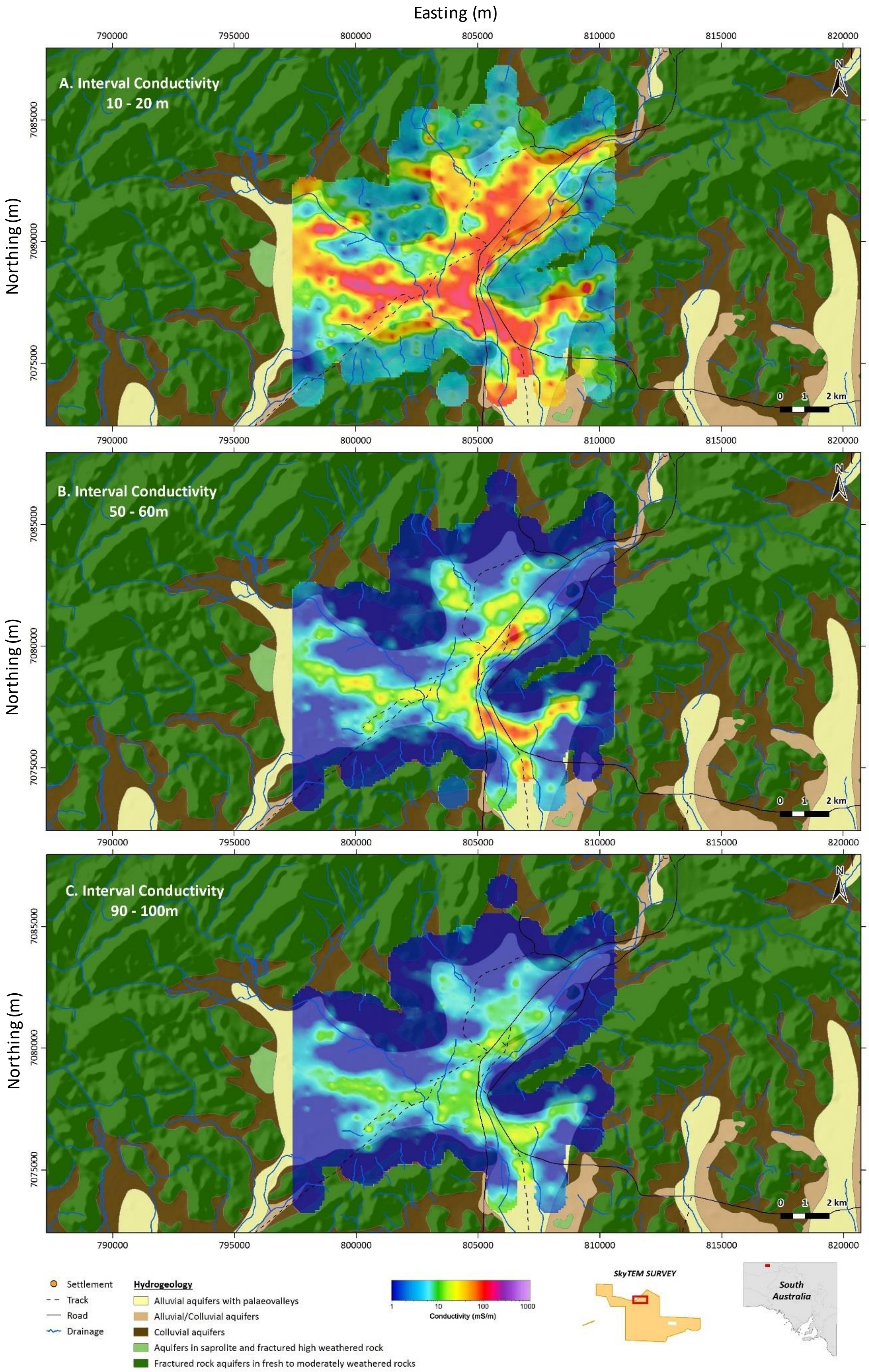

Figure 30. SkyTEM spatially constrained inversion (SCI) interval conductivities for the infill area south-east of Pukatja. Intervals are overlain on hydrogeological framework map.

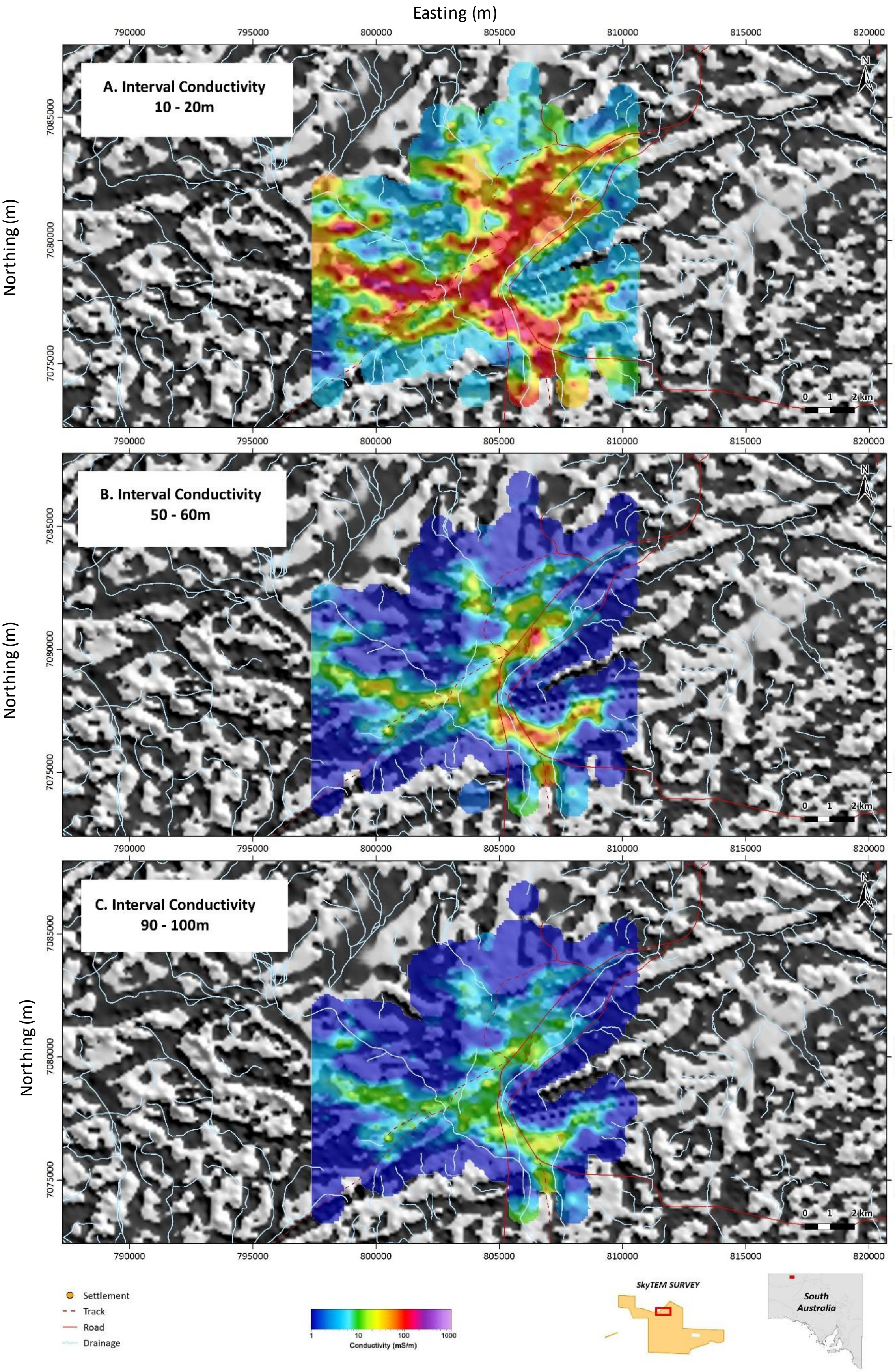

Figure 31. SkyTEM spatially constrained inversion (SCI) interval conductivities for the infill area south-east of Pukatja. Intervals are overlain on first vertical derivative (1VD) magnetic greyscale image.

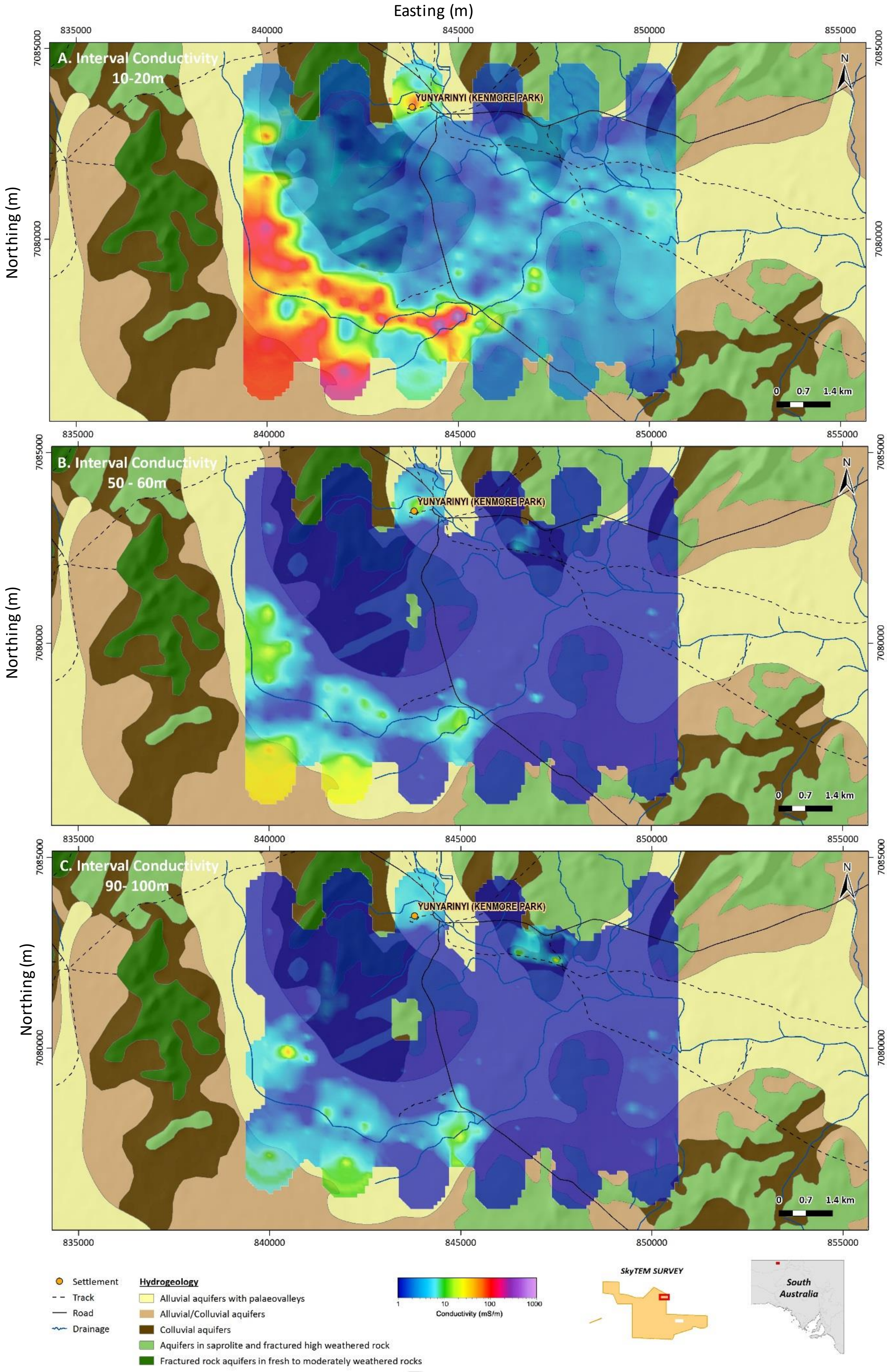

Figure 32. SkyTEM spatially constrained inversion (SCI) interval conductivities for the infill area south of Yunyarinyi. Intervals are overlain on hydrogeological framework map.

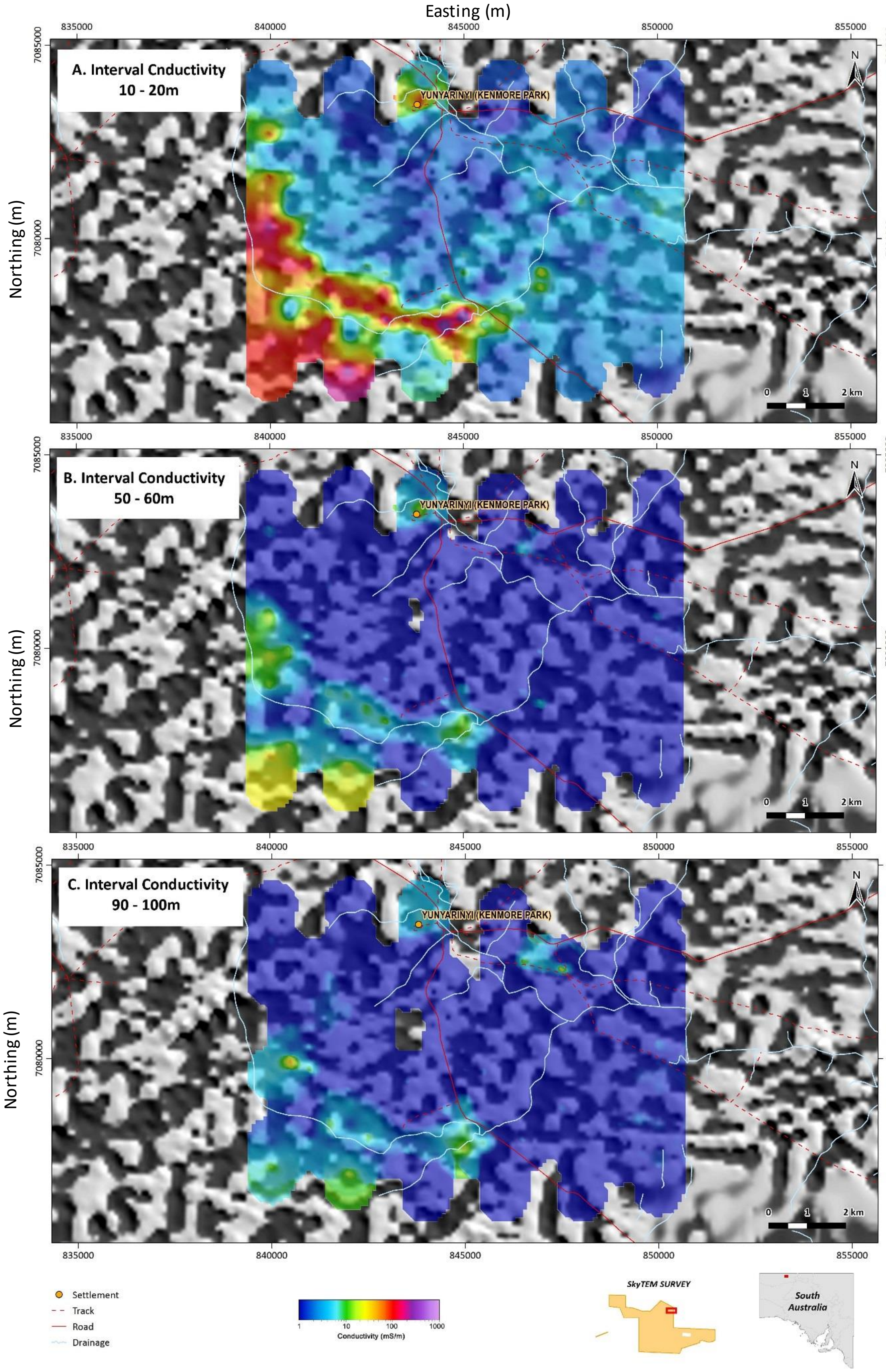

Figure 33. SkyTEM spatially constrained inversion (SCI) interval conductivities for the infill area south-east of Yunyarinyi. Intervals are overlain on first vertical derivative (1VD) magnetic greyscale image.

.

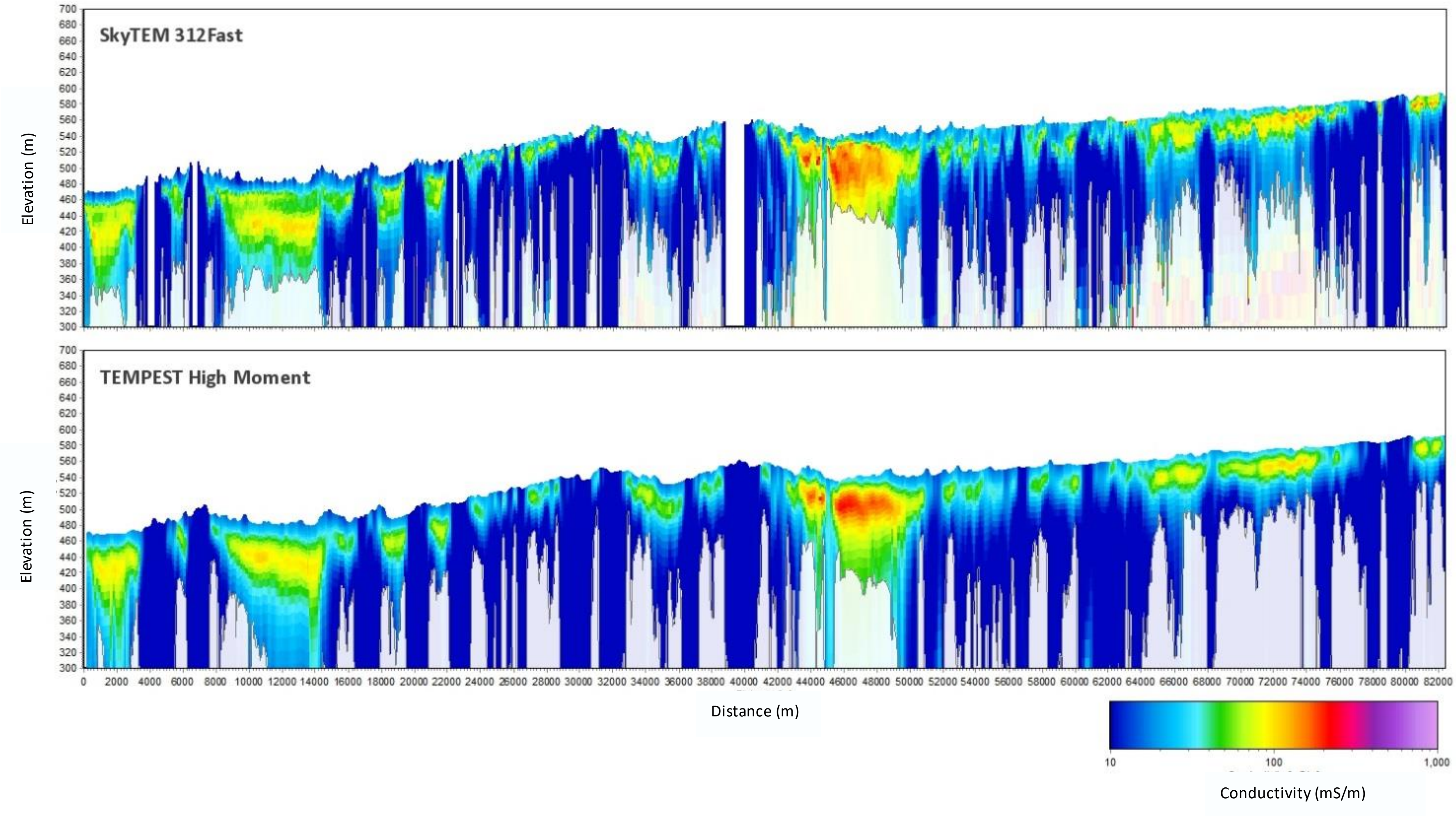

Figure 34. Conductivity-depth section for coincident flight lines of the SkyTEM (top panel) and TEMPEST (lower panel) airborne electromagnetic systems in the central part of the Musgrave Province. The depth of investigation is indicated by the opaque white area in the lower part of the sections shown.

6 Summary

The conductivity structure of the Musgrave Province has been defined through the processing and inversion of two regional AEM data sets that were acquired by the South Australian Government through the Goyder Institute and the Geological Survey of South Australia as part of the G-Flows project and the PACE Cu initiative. Two, time domain AEM systems were employed in the regional surveys – the fixed wing TEMPEST High Moment and rotary wing SkyTEM^{312FAST}. Inversion results indicate that both systems effectively define the cover, which is relatively conductive, and map buried palaeovalley systems in this area, particularly their location and geometry. The interpretation of the inversion products forms part of a separate study on the conceptualisation of the hydrogeology of the region. The correspondence between the alluvial units defined in the hydrogeological framework map and the more electrically conductive parts of the landscape, particularly the deeper conductive structure (interpreted to represent palaeovalley sediment fill) indicates the robustness of the hydrogeological conceptualisation developed in G-Flows Stage-1 (see Munday et al. 2013).

Definition of the spatial complexity (at a regional scale) of the cover will enhance our understanding of the region's groundwater resource potential; important for communities, industry and the environment. The initial results also indicate a potential to map variations within the palaeovalley systems themselves, something that will be useful for assisting in locating compartmentalised aquifers particularly in areas with limited drilling. Gaining an understanding of the cover thickness and spatial variability will also help reduce exploration risks in the area.

The effects of airborne IP are apparent in the two data sets, and further work is required to address its significance in defining cover variability, particularly as it affects the derived conductivity structure. Nonetheless, the preliminary inversion results can form a reliable basis for planning follow-up ground investigations in the region.

7 Conclusion

The inverted products of two regional AEM surveys, acquired by different systems, have been merged to provide a regional-scale image of the palaeovalley systems that characterise the Musgrave Province. The orientation and distribution of the palaeovalley fill is represented as a conductive sedimentary sequence, which overlies a very resistive basement. The derived conductivity structure appears well determined by a 1D layered earth inversion. The conductivity pattern and by inference, the palaeovalleys shows a close affinity with the basement structure of the province, indicating its significance in determining the original drainage systems. The observed conductivity structure also shows a close correspondence with the alluvial sequences defined in the GFLOWS-1 hydrogeological framework map, indicating that the original conceptualisation, based on combining information from a contemporary terrain index (MrVBF: Gallant and Dowling 2003) and local-scale airborne electromagnetic data acquired for mineral exploration in the region, was well founded.

References

Auken, E. and Christiansen, A. V., 2004, Layered and laterally constrained 2D inversion of resistivity data. *Geophysics*, 69, 752-761.

Auken, E., Christiansen, A. V., Jacobsen, Bo. H., Foged, N., and Sørensen, K.I., 2005, Piecewise 1D laterally constrained inversion of resistivity data. *Geophysical Prospecting*, 53, 497–506.

Auken, E., Christiansen, A. V., Kirkegaard, C., Fiandaca, G., Schamper, C., Behroozmand, A. A., Binley, A., Nielsen, E ., Effersø, F., Christensen, N. B., Sørensen, K., Foged, N. and Vignoli, G., 2015, An overview of a highly versatile forward and stable inverse algorithm for airborne, ground-based and borehole electromagnetic and electric data. *Exploration Geophysics*, 46, 223–235.

Beckitt, G., 2003, Exploration for unconformity uranium in Arnhem Land (NT). *Exploration Geophysics*, 34, 137–142.

CGG, 2016, High Moment TEMPEST Geophysical Survey Musgrave Region – PACE Components Airborne EM Survey, South Australia. Logistics and Processing report.

Chen, J. and Raiche, A., 1998, Inverting AEM data using a damped eigen parameter method. *Exploration Geophysics*, 29, 128–132.

Christensen, N.B., 2002, A generic 1-D imaging method for transient electromagnetic data. *Geophysics*, 67, 438-447.

Christiansen, A.V. and Auken, E., 2012, A global measure for depth of investigation. *Geophysics*, 77, WB171–WB177.

Craig, M.A. ed., 2011, Geological and energy implications of the Pine Creek region airborne electromagnetic (AEM) survey, Northern Territory, Australia. Geoscience Australia Record 2011/18, 292.

Davis, A.C., Munday, T.J. and George, R.J., 2015, Gascoyne River airborne electromagnetic survey II: Inversion Report. CSIRO: Water for a Healthy Country Flagship Technical Report; CSIRO Technical Report EP-13-11-758. 158pp.

Davis, A.C., Macaulay, S., Munday, T.J., Sorensen, C., Shudra, J., and Ibrahimi, T. 2016, Uncovering the Groundwater Resource Potential of Murchison Region in Western Australia Through Targeted Application of Airborne Electromagnetics. ASEG Extended Abstracts 2016, 1-6. https://doi.org/10.1071/ASEG2016ab307

Farquharson, C.G. and Oldenburg, D.W., 1998, Non-linear inversion using general measures of data misfit and model structure. *Geophysical Journal International*, 134, 213–227.

Fitzpatrick, A., Munday, T.J., Cahill, K., and Stelfox, L., 2011, A regional, reconnaissance scale AEM survey to aid the definition of surface water - groundwater processes beneath a large unregulated river system: Fitzroy River, Western Australia. CSIRO Technical Report No: CESRE P2010/1235.

Flis, M.F., Newman, G.A., and Hohmann, G.W., 1989, Induced-polarization effects in time-domain electromagnetic measurements. *Geophysics*, 54, 514–523.

Gallant, J.C. and Dowling, T.I., 2003, A multiresolution index of valley bottom flatness for mapping depositional areas. *Water Resources Research*, 39, 1347.

Halkjaer, M., Sorensen, K.I., Christiansen, N.B., and Auken, E., 2006, SkyTEM – Status and development. Australian Earth Sciences Convention 2006, Melbourne, Australia.

Lane, R. and Pracilio, G., 2000, Visualisation of Sub-Surface Conductivity Derived From Airborne EM. SAGEEP 2000 Conference Proceedings.

Lane, R., Green, A., Golding, C., Owers, M., Pik, P., Plunkett, C., Sattel, D., and Thorn, B., 2000, An example of 3D conductivity mapping using the TEMPEST airborne electromagnetic system. *Exploration Geophysics*, 31, 162–172.

Lane, R., Heislers, D., and McDonald, P., 2001, Filling in the gaps – validation and integration of airborne EM data with surface and subsurface observations for catchment management – an example from Bendigo, Victoria, Australia. *Exploration Geophy*sics, 32, 205–215.

Lane, R., Brodie, R., and Fitzpatrick, A., 2004, Lower Balonne airborne geophysical project – Constrained inversion of AEM data from the lower Balonne area, Southern Queensland, Australia. CRC LEME Open File Report 163.

Lawrie, K.C., Clarke, J.C., Tan, K.P., Munday, T.J., Fitzpatrick, A., Brodie, R.S., Pain, C.F., Apps, H., Cullen, K., Halas, L., Kuske, T.J., Cahill, K., and Davis, A., 2010, Using the SkyTEM time domain airborne electromagnetics (AEM) system to map aquifer systems and salinity hazard in the Ord Valley, Western Australia: Geoscience Australia Professional Opinion 2010/01.

Ley-Cooper, A.Y., Munday T.J., and Ibrahimi, T., 2017, Inversion of the Capricorn Orogeny regional Airborne Electromagnetic (AEM) survey, Western Australia. CSIRO Technical Report EP166290, pp. 37.

Macnae, J., King, A., Stolz, N., Osmakoff, A., and Blaha, A., 1998, Fast AEM data processing and inversion. *Exploration Geophysics*, 29, 163–169.

Macnae, J., 2007, Developments in broadband airborne electromagnetics in the past decade. In Proceedings of Exploration 07: Fifth Decennial International Conference on Mineral Exploration" edited by Milkereit, B., 387-398.

Munday, T., Abdat, T., Ley-Cooper, Y., and Gilfedder, M., 2013, Facilitating Long-term Outback Water Solutions (G-FLOWS Stage-1): Hydrogeological Framework. Goyder Institute for Water Research Technical Report Series No. 13/12.

Munday, T.J., Sorensen, C.C., Ibrahimi, T., and Cahill, K., 2016, SARFIIP Salinity Investigations: Katfish SkyTEM AEM Geophysical Survey: Processing and Interpretation Final Report. Report Number EP159200, 71pp, CSIRO, Australia.

Newman, G.A., Anderson, W.L., and Hohmann, G.W., 1987, Interpretation of transient electromagnetic soundings over three-dimensional structures for the central-loop configuration. *Geophysical Journal of the Royal Astronomical Society*, 89, 889–914.

Reid, J.E., Pfaffling, A.. and Vrbancich, J., 2006, Airborne electromagnetic footprints in 1D earths. *Geophysics*, 71(2), G63–G72. doi: 10.1190/1.2187756.

Roach, I.C. ed., 2010, Geological and energy implications of the Paterson Province airborne electromagnetic (AEM) survey, Western Australia. Geoscience Australia Record 2010/12, 318.

Roach, I.C., ed., 2012. The Frome airborne electromagnetic survey, South Australia: implications for energy, minerals and regional geology. Geoscience Australia Record 2012/40 – DMITRE Report Book 2012/00003, 296 pp.

Sattel, D., 1998, Conductivity information in three dimensions. *Exploration Geophysics*, 29, 157–162.

Sattel, D., 2005, Inverting airborne electromagnetic (AEM) data with Zohdy's method. *Geophysics*, 70(4), G77–G85.

Sattel, D. and Kgotlhang L., 2004, Groundwater exploration with AEM in the Boteti Area, Botswana. *Exploration Geophysics*, 35, 147-156.

Sengpiel, K.P. and Siemon, B., 2000, Advanced inversion methods for airborne electromagnetic exploration. *Geophysics*, 65, 1983–1992.

SkyTEM, 2016, SkyTEM helicopter EM survey Musgrave Region – (CSIRO Components), SA 2016, Acquisition and processing report.

Smith, R.S., 1989, Discussion on: "Induced polarization effects in time domain electromagnetic measurements". *Geophysics*, 54, 514–523. doi: 10 .1190/1.1442678.

Smith, R.S., 2016, Induced-polarization effects in airborne electromagnetic data: Estimating chargeability from shape reversals. SEG Technical Program Expanded Abstracts, pp. 2211–2217.

Sørensen, K.I. and Auken, E., 2004, SkyTEM - A new high-resolution helicopter transient electromagnetic system. *Exploration Geophysics*, 35, 191–199.

Soerensen, C. and Munday, T.J., 2018, The Musgrave Province – the untold story about Airborne IP. Extended Abstract, AEM 2008/7th International Workshop on Airborne Electromagnetics, June 17-20, Kolding, Denmark, 4pp.

Viezzoli, A., Auken, E., and Munday, T.J., 2009, Spatially constrained inversion for quasi 3D modelling of airborne electromagnetic data – an application for environmental assessment in the Lower Murray Region of South Australia. *Exploration Geophysics*, 40, 173–183.

Viezzoli, A., Kaminski, V., and Fiandaca, G., 2017, Modeling induced polarization effects in helicopter time-domain electromagnetic data: Synthetic case studies. *Geophysics*, 82(2), E31–E50. doi: 10.1190/geo2016-0096.1

Watt E.L. and Berens V., 2011, Non-prescribed groundwater resources assessment – Alinytjara Wilurara Natural Resources Management Region. Phase 1 – Literature and Data Review, DFW Technical Report 2011/18, Government of South Australia, Department for Water, Adelaide.

The Goyder Institute for Water Research is a partnership between the South Australian Government through the Department for Environment and Water, CSIRO, Flinders University, the University of Adelaide, the University of South Australia, and the International Centre of Excellence in Water Resource Management.